

## Mesoscale modelling of concrete – A review of geometry generation, placing algorithms, constitutive relations and applications



P.S.M. Thilakarathna<sup>a</sup>, K.S. Kristombu Baduge<sup>a</sup>, P. Mendis<sup>a,\*</sup>, V. Vimonsatit<sup>b</sup>, H. Lee<sup>b</sup>

<sup>a</sup> Department of Infrastructure Engineering, University of Melbourne, Victoria, Australia

<sup>b</sup> Department of Civil Engineering, Curtin University, Western Australia, Australia

### ARTICLE INFO

#### Keywords:

Mesoscale modelling  
Discrete element method  
Lattice element method  
Rigid body spring method  
Lattice discrete particle method  
Finite element analysis

### ABSTRACT

Concrete can be considered as a heterogeneous material at mesoscale comprising of several constituents such as aggregates, mortar and Interfacial Transition Zone (ITZ). Mechanical behavior as well as the durability characteristics of concrete is highly dependent on the mesostructure of concrete and investigating the complex phenomena surrounding concrete at mesoscale considering the heterogeneity presents an important tool to understand these complex mechanisms. Presenting the state-of-the-art developments in mesoscale modelling of concrete considering different analysis methods such as continuum Finite Element Modelling (FEM), Lattice Element Method (LEM), Rigid Body Spring Method (RBSM), Discrete Element Method (DEM) and Lattice Discrete Particle Method (LDPM) is the focus of this review paper. Effective methods to generate the geometry of consisting phases in the mesoscale models including different particle shapes and placing algorithms, selecting suitable material constitutive relations for the consisting phases are discussed for these different methods of mesoscale modelling. Potential applications including fracture mechanics and strengths and weaknesses of each technique are highlighted with possible methods to overcome the challenges of mesoscale modelling of concrete.

### 1. Introduction

Concrete can be modelled and understood considering it as a multiscale material consisting of different scales such as macroscale, mesoscale and microscale as shown in Fig. 1 [1]. Macroscale of concrete is considered as homogeneous, but internally concrete is heterogeneous in nature. Mesoscale models are widely used to understand the mechanical properties and failure mechanisms of concrete, contribution of its phases to the behavior and to obtain homogenized responses in macroscale accurately while considering the heterogeneous properties. Mesoscale modelling of concrete provides a unique method to investigate the complex damage initiation of microcracks, coalescence of these microcracks to form major cracks contributing to the failure of concrete [2] and also the localized deformations which cannot be captured using continuum homogeneous models. In order to comprehensively comprehend the failure process of concrete, inherent heterogeneous nature of concrete needs to be considered and mesoscale modelling has proven to be the most effective way of understanding the fracture behavior due to its capability of modelling these heterogeneities [3,4]. Macroscale simulations have the drawback of lack of accurate material models to represent the actual nonlinear behavior of the

\* Corresponding author.

E-mail address: [pamendis@unimelb.edu.au](mailto:pamendis@unimelb.edu.au) (P. Mendis).

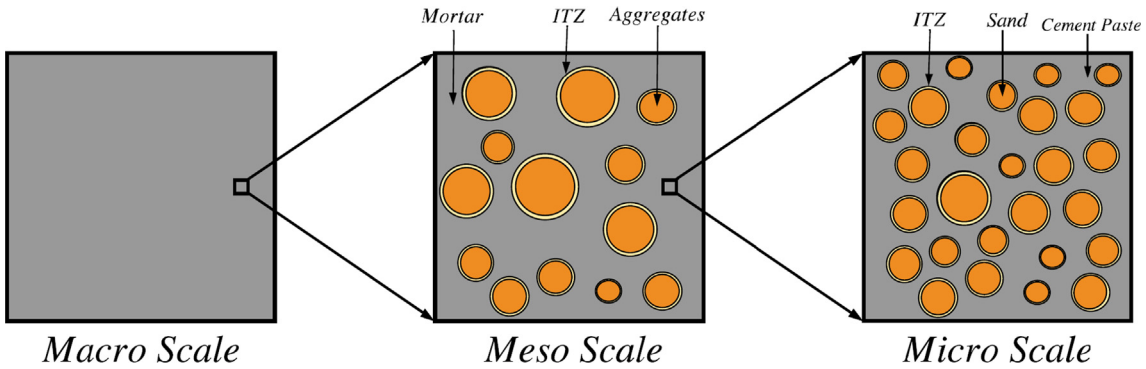


Fig. 1. Multiscale of concrete [1].

concrete when constituent materials (phases) are changed. However, by using the mesoscale models, homogenized response can be obtained for different mix proportions by assigning the known material models for the components of mesoscale [5]. In the mesoscopic level, concrete is modelled as a composite material consisting of three phases of ITZ, coarse aggregates and mortar matrix. ITZ properties vary substantially from the mortar matrix due to the gradient of porosity and the complementary gradient of anhydrous cement [6] and hence, it is important to model these phases separately in the mesoscale models [7].

Mesoscale models can be used effectively to study the effect of concrete mix on the macro properties of concrete and to investigate the nonlinear behaviour of concrete [8]. It is the most useful and practical way of modelling concrete when the heterogeneous nature of concrete should be taken into account in order to understand how the phases affect the macro behavior, fracture mechanics of concrete and how to improve the performance of concrete. By using mesoscale models to simulate the behavior of concrete, number of experimental tests can be reduced [9]. For experimental procedures, significant amount of expenses and time is spent and through numerical modelling, this can be reduced. Comby-Peyrot [10] suggested that modelling the heterogeneities of concrete is important to model the damage initiation and progression, investigate about various concrete formulations, investigate local deformation mechanisms and study the chemical degradation in concrete. Therefore, meso-scale modeling with accurate constitutive material behavior can be considered as cost-effective, and time effective alternative to predict mechanical behavior and optimum mix design method for concrete.

Mesoscale modelling can be mainly divided into two segments as continuum mesoscale modelling and discrete mesoscale modelling depending on the analysis procedure. Continuum mesoscale modelling represents the mesostructure of concrete as a continuum and mainly uses finite element method for the analysis. Discrete mesoscale modelling represents the concrete mesostructure using distinct elements such as spheres, lattice beams, trusses etc. There are many pros and cons for each mesoscale analysis technique, and it is important to have a thorough understanding about the strengths and weaknesses of these different techniques before choosing a method.

In this paper, a comprehensive review of mesoscale modelling of concrete including geometry generation, placing algorithms, material constitutive relations and applications in fracture mechanics, concrete durability investigations, nonlinear concrete modelling etc. will be carried out with the comparison of continuum methods and discrete methods. The objective of this paper is to critically evaluate continuum and discrete mesoscale modelling techniques with their strengths, weaknesses, applications and the challenges in modelling and methods to overcome those challenges.

## 2. Generation of geometry for meso-scale - continuum method

In the continuum method, concrete mesostructure is represented as a continuum with aggregates, mortar and ITZ when concrete is modelled as a three-phase material and with aggregates and mortar when concrete is represented as a two-phase material. Generally, there are two methods to generate geometry in the continuum mesoscale modelling. First one is using the digital image based approach which uses image-processing techniques and the other method is generating the mesostructure through parameterization modelling [11]. These two methods are further discussed in the following sections.

### 2.1. Digital image based approach

In this method, digital images of the concrete specimen are taken and using image processing techniques, these images are processed, and the mesoscale model is generated [12]. This approach can be used to create the concrete mesostructure with a great extent of accuracy. There are two main approaches to generate the images of the concrete specimen. In the first method, concrete specimen is scraped and 2D images are taken using a scanner and these images are combined to get the full 3D geometry of the concrete specimen [13].

Second method uses scanning of an actual concrete cube using X-ray computed tomography (XCT) scanners and generate mesh using the digitally scanned elements [14–22] as shown in Fig. 2. This method is a non-destructive method of generating the mesostructure [23] and this can identify the different components of a material. It can also be used to visualize the materials because of

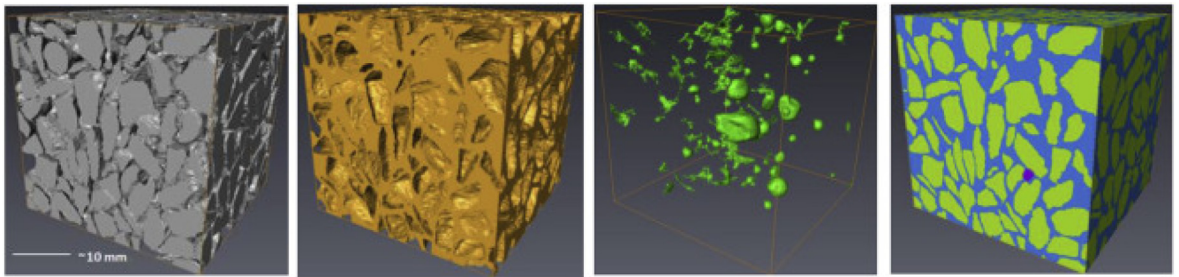


**Fig. 2.** Mesostructure generation using CT scanning process [25].

the clear 3D visualizations and high resolution image generation [18]. From this method, a continuum mesh of the mesostructure can be generated by either using boundary detection techniques or using voxel methods. In boundary detection technique, boundaries of the consisting phases of mesostructure are identified using image processing and then these boundaries are meshed using a meshing software and in voxel method, each pixel is mapped to a hexahedral element to generate the mesh [24].

Li and Li [23] generated the images of the specimen using a medical CT scanner and processed the images to obtain the final mesostructure of the concrete. However, in this scenario, some of the aggregate geometries were overlapped due to the inability to properly identify and differentiate the boundary of the particles. Also, the generated mesh needs to be simplified to reduce the demand for the computational resources.

Using the digital image-based approach, complete verification of the developed mesoscale mode can be done because the generated mesoscale aggregate model is geometrically similar to the actual experimental specimen [26]. However, generating the mesostructure is time consuming and costly. Also, there should be large number of samples for statistical analysis and this is not feasible with this method. Another drawback is that when the volume rendering is done by stacking the obtained 2D images, resolution of the horizontal and vertical directions will be different because the spacing of the 2D images is larger compared with the image resolution [17].

Schematic diagram of a basic XCT system is shown in Fig. 3. Concrete sample is mounted on the turntable and the turntable is rotated step by step and after a step, radiograph projections are captured [27]. Resolution of the scan is dependent on the distance between detector and sample, distance between the X-ray source and the sample, size of the X-ray source and spacing and dimensions of the detector elements [28].

Image resolutions, field of view and the sample sizes used by different researchers are listed in Table 1. Pixel size should be small enough to capture the geometry of the heterogeneities in the mesostructure and if the pixel size is too small, the number of elements will be increased, the size of an individual finite element will be reduced, and the simulation time will be increased. Generally, each pixel will be modelled by a quadrilateral element in 2D or a voxel in 3D in finite element simulations. However, it should be noted that using this resolution, representing the actual thickness of ITZ which is around 10–50  $\mu\text{m}$  is unrealistic and hence an ITZ thickness around 0.1–0.4 mm is widely used [19,26]. Even in this scenario, the interface between the mortar and the aggregate will be in a zigzag shape and it does not represent the real material interface well. Also, the stress concentrations in corner points might lead to

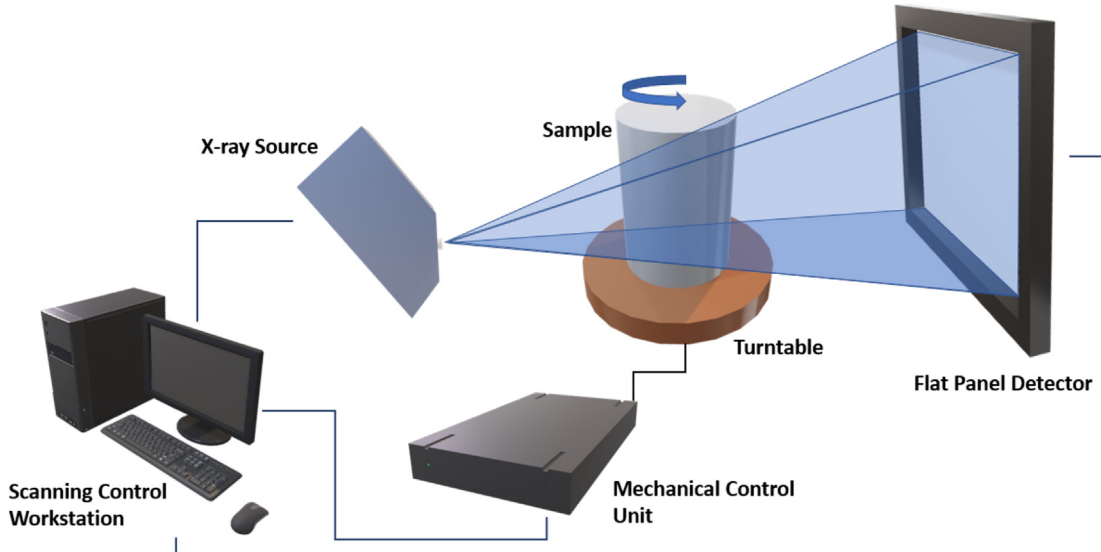


**Fig. 3.** Schematic diagram of XCT system.

**Table 1**

Image resolutions, field of view and sample size.

Reference	Resolution	Field of View	Sample Size
Yang et al. [12]	0.1 mm/pixel	37.2 mm	40 mm × 40 mm × 40 mm
Huang et al. [19,22,26]	0.1 mm/pixel	37.2 mm	40 mm × 40 mm × 40 mm
Wang et al. [17]	Horizontal – 0.3 mm/pixel Vertical – 0.2 mm/pixel	–	–
Ren et al. [18]	0.1 mm/pixel	37.2 mm	40 mm × 40 mm × 40 mm

difficulties in finite element simulations [18].

It can also be seen from Table 1, that smaller sample sizes should be used in this scenario due to the restrictions of field of view. Apart from generating the accurate representation of the mesostructure of the concrete, XCT can be used to do in-situ imaging of concrete. Using this method, fracture and damage initiation and progression can be observed with time and also these results can be used to validate the numerical mesoscale models [12]. These in-situ scanned models can be considered as representative volume elements which include the mesoscale heterogeneities. However, if the overall fracture behavior of the sample needs to be observed, a larger volume needs to be modelled and this can be achieved using parameterization approach.

## 2.2. Parameterization modelling approach

In the parameterization approach, concrete mesostructure is generated using algorithms which represent the geometry of the mesostructure parametrically. Aggregates will be represented using various shapes and these aggregates will be placed inside a volume and the mortar phase is represented by the volume surrounding the already placed aggregates. Generation of the mesoscale models including shape generation of aggregates, methods to obtain optimum Particle Size Distribution (PSD), aggregate placing methods, generation of ITZ, and meshing techniques are discussed in this section.

### 2.2.1. Shape of aggregates

First step in the process of generating the mesostructure using parameterization modelling approach is the generation of aggregate particles. Different shapes such as spherical, ellipsoidal and polyhedral have been used to represent the aggregates in 3D and planer shapes like polygons, ellipses and circles are used to represent aggregates in 2D [29]. In this paper 3D aggregate generation is focused because generation of 2D shapes is straightforward. Spherical shape is a widely used aggregate shape due to the convenience in particle shape generation [8,30,31]. Spheres are uniquely represented in 3D space by the center coordinates and the radius of the particles.

Ellipsoids have also been used to represent the aggregate particles in mesoscale concrete modelling. Ellipsoids can be represented uniquely in 3D space using nine parameters. Those parameters are lengths of the three middle axes of the ellipsoid, three center coordinates and the three Eulerian angles. However, spherical and ellipsoidal particle shape does not realistically represent the stress concentrations of the angular corners of the crushed aggregates.

Häfner et al. [32] proposed to add a sine function to the spherical and ellipsoidal formulations so that the final aggregate surface is nonuniform. Qian [33] developed irregular shaped aggregate particles using spherical harmonic functions. Irregular shape of the particle is uniquely defined using a set of spherical harmonic coefficients. Using these irregular particle shapes, particles shapes similar to the actual aggregate shapes in concrete can be achieved. These irregular shaped particles which are developed using the spherical harmonic functions and distributed using take and place method are illustrated in Fig. 4. Mazzucco et al. [34] used a laser

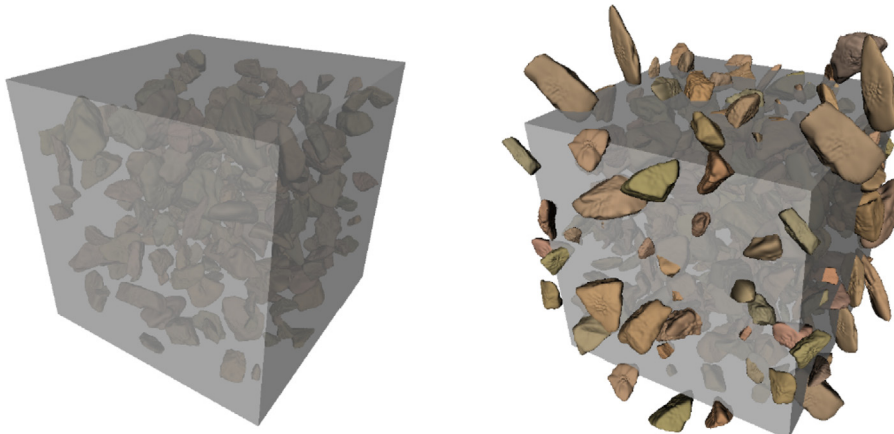
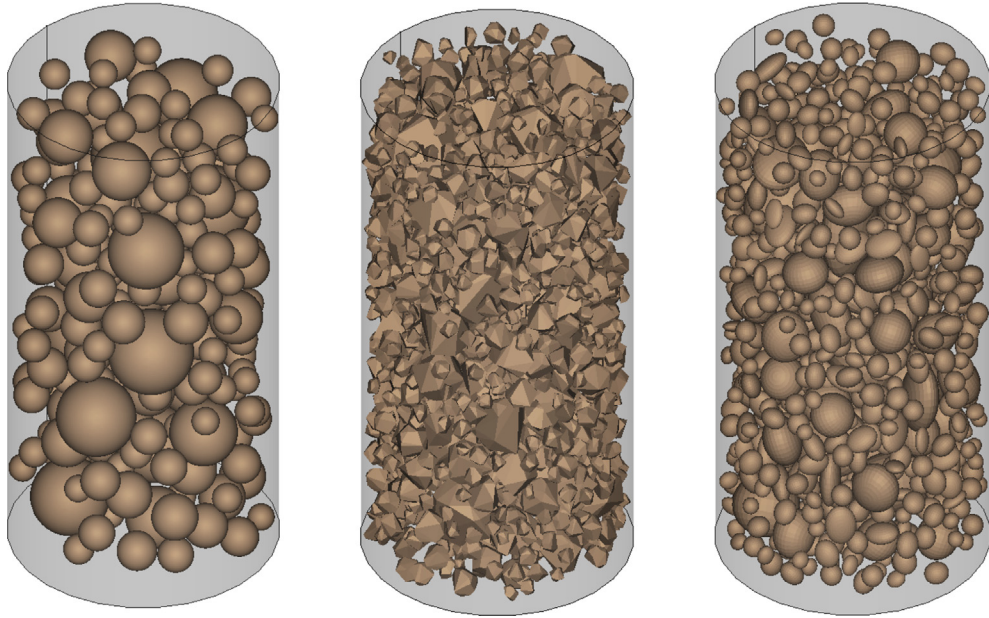


Fig. 4. Irregular aggregate particles [33].



**Fig. 5.** Generated spherical, polyhedral and ellipsoidal particles.

scanner to generate the accurate form of aggregate particles to be used in the mesoscale model and these laser scanned particles were simplified using a CAD software to simplify the computational efforts. Zhou et al. [35] also used the laser scanning technique to scan aggregate particles to obtain the real shape and used spatial random cutting technique to generate 2D aggregate shape library.

Using ellipsoids and spheres to represent uncrushed aggregate such as pea-gravel particles with smooth surfaces is realistic. However, the crushed aggregate particles have rough surface, flaky shape and elongated surfaces [36]. Polyhedrons have been used to represent the actual aggregate shape of the crushed aggregate particles [37]. Due to the angular nature of aggregate particles, local stress concentrations will occur, and these will lead to the crack initiation [38] and polyhedral particles can realistically represent this behavior. Zhang et al. [39,40] developed a 3D Voronoi diagram and shrunk it to develop the polyhedral aggregate particle shape. Zhou et al. [41] generated aggregates with polyhedral shape using random points in the space. These random points were bound using a convex hull and flaky and elongated aggregate shapes were generated using a shrinkage and expansion ratio. Generated aggregate particles inside a cylinder using authors own code is shown in Fig. 5. Take and place method was used particle distribution in this scenario,

#### 2.2.2. Particle size distribution (PSD) of aggregates

Aggregate distribution is an important aspect in continuum mesostructure generation as this will affect the mechanical properties and behavior including fracture [42]. Most of the researchers have used Fuller's curve [43] to obtain the PSD curve for the mesoscale modelling of the concrete [8,30,39,44–47]. Fuller's curve is widely accepted as the grading curve which gives the optimum compaction, density and strength in concrete and also a good workability and a good segregation resistance [8]. According to the Fuller's curve, aggregate percentage by weight passing through a sieve diameter D is given by Eq. (1).

$$Y = 100 \left( \frac{D}{D_{max}} \right)^{1/2} \quad (1)$$

In the above equation, Y is the percentage of aggregate by weight passing through a sieve with diameter D aperture and  $D_{max}$  is the diameter of the largest aggregate.

Instead of using experiment-based PSD curves such as Fuller's curve, code based particle size distribution curves such as PSD given in EN 933-1 have also been used to obtain the aggregate breakdown in mesoscale modelling [10].

#### 2.2.3. Aggregate placing algorithms

After generating the aggregate particles, aggregate placement is done inside the volume. Generally, three conditions need to be satisfied when placing the aggregate particles: 1. aggregates should be completely inside the bounding volume; 2. there should not be any overlaps between aggregate particles; and 3. there should be a minimum distance between two aggregate particles because there should be a coating of mortar in between aggregate particles. For this coating thickness, Schlangen and van Mier [48] proposed to use  $0.1(d_1 + d_2)$  where  $d_1$  and  $d_2$  are the diameters of the two aggregate particles. Wang et al. [36] proposed to use a thickness of  $\gamma D$  where D is the smaller particle diameter of the adjacent two particles and  $\gamma$  is a constant. This will make sure that the mortar coating in between two aggregate particles are proportional to the aggregate size, smaller particles are placed closer to the large particles and

even distribution of large particles. Generally, the third condition is checked with the first two conditions for the spherical particles.

For spherical particles, addition of two radii of the aggregates should be less than the distance between the centers of the aggregate particles to avoid the overlap of the particles. If the minimum distance between two aggregates is  $[r_A + (1 + 2\gamma)r_B]$  where  $\gamma$  is a constant and  $r_A$  is the radius of the larger particle and  $r_B$  is the radius of the smaller particle, third condition is automatically checked. Value of the constant  $\gamma$  is important because if a higher value is used, uniform aggregate distribution can be obtained but it might be difficult to obtain the preferred aggregate fraction. Satisfying these conditions are comparatively difficult for the particles with ellipsoidal and polyhedral shape than the spherical particles because it requires a much more complex algorithm which costs in computation time.

Checking the overlapping criteria for the ellipsoids are more challenging compared with the spherical aggregates. Wang et al. [49] proposed an algebraic method to check the overlapping of the ellipsoidal particles. If  $p$  and  $q$  are two ellipsoidal particles, those two ellipsoids can be represented by  $X^T Q_p X = 0$  and  $X^T Q_q X = 0$  where  $Q_p$  and  $Q_q$  are the coefficient matrices of the two ellipsoids and  $X = (x, y, z, w)$  are the homogeneous coordinates of points  $(\frac{x}{w}, \frac{y}{w}, \frac{z}{w}) \in R^3$ . It has been proved that the two ellipsoids do not overlap if the their characteristic equation  $f(\lambda) = \det(\lambda Q_p + Q_q) = 0$  has two distinct positive roots. Coefficient matrix of the ellipsoid can be obtained using Eq. (2).

$$Q = \begin{bmatrix} A & D & F & G \\ D & B & E & H \\ F & E & C & I \\ G & H & I & J \end{bmatrix} \quad (2)$$

where A, B, C, D, E, F, G, H, I are the coefficients in the quadratic ellipsoid equation,

$$F(x, y, z) = Ax^2 + By^2 + Cz^2 + Dxy + Exz + Fyz + Gx + Hy + Iz + J \leq 0 \quad (3)$$

Bailakanavar et al. [50] proposed a method to check whether two convex 3D shapes intersect. This method contains three steps. These steps are in the order of increasing the demand for computational capacity. First step is to check the distance between the two centers of the ellipsoid which includes the 3D convex polygon. If this distance is less than the maximum diameter of the semi principal axes, the particles do not overlap. Second step is to check intersection using the method of separating planes and the final step is to check the intersection using method of separating axes. Method of separating planes involves checking whether any node inside the shape lies inside or on the other shape and method of separating axes involves checking whether any lines in two shapes projected on to a reference line called ‘separating axis’ intersect [50].

Aggregate placement in the volume has been done using various methods. Most widely used method is the take and place method [36,48,51,52]. In this method, particles are placed in the volume from largest particle to smallest particle until the specified volume fraction is achieved. Placing the aggregates in the volume starting from the largest particle rather than from the smallest particle drastically improves the efficiency of the particle placing algorithm [32]. Particles are placed using the coordinates generated by a random number generator and placed particles are checked for overlaps and gaps between the aggregates. This method is a simple and convenient method. Placement of the final few particles will take a long time because the probability of overlapping particles at this stage is higher. Process of generating a cylinder with spherical aggregate particles for a given volume fraction using take and place method is shown in Fig. 6.

In that process, first the particle size distribution curve (e.g. Fuller’s curve) is divided in to segments and the volume of particles in that grading segment is calculated using Eq. (4).

$$V_p [d_s, d_{s+1}] = \left( \frac{P(d_s) - P(d_{s+1})}{P(d_{max}) - P(d_{min})} \right) \times v_p \times V \quad (4)$$

where  $V_p [d_s, d_{s+1}]$  is the volume of aggregate within the grading segment  $[d_s, d_{s+1}]$ ,  $d$  is the sieve diameter,  $d_{max}$  and  $d_{min}$  are the largest and smallest sieve diameter  $v_p$  is the volume fraction of aggregates,  $P(d)$  is the cumulative percentage passing a sieve with aperture diameter  $d$  and  $V$  is the total volume of the concrete.

Leite, Slowik and Mihashi [53] proposed a stochastic-heuristic algorithm for placing the aggregate particles in the volume. Ellipsoidal particles were used to represent aggregates. Particles are initially placed inside the volume using random numbers for the center point coordinates and the axes directions. If the particle overlaps with previously placed particles or it is not completely inside the box, particles are moved using the stochastic-heuristic algorithm with rotations and translations. This algorithm is similar to the real concrete placing process as smaller particles are adjusted by bouncing back with the larger particles. Representation of this algorithm is shown in Fig. 7.

Wrighers and Moftah [8] used a similar approach where if two particles overlap, translations and rotations of the particle is done to avoid the overlapping. Zhou et al. [41] used translations and rotations to avoid overlapped polyhedral particles and observed that this will reduce the computing time approximately by 60% and also increase the particle volume fraction by about 4%.

Du and Sun [54] proposed random extension method to distribute arbitrarily shaped aggregates into a 3D volume. In this method all aggregates are placed at once rather than placing aggregates one by one checking the overlapping conditions. Tetrahedral and hexahedral aggregates are used as the fundamental shapes for initial aggregate generation in a sphere. Then these fundamental aggregates are extended to increase the volume fraction as shown in Fig. 8.

Zhang et al. [29] proposed a method called ‘random walking algorithm’ where aggregates are first placed in an initial placing domain and then moved into the target placing domain. This placing method realistically represents the actual concrete placing behavior in a concrete.

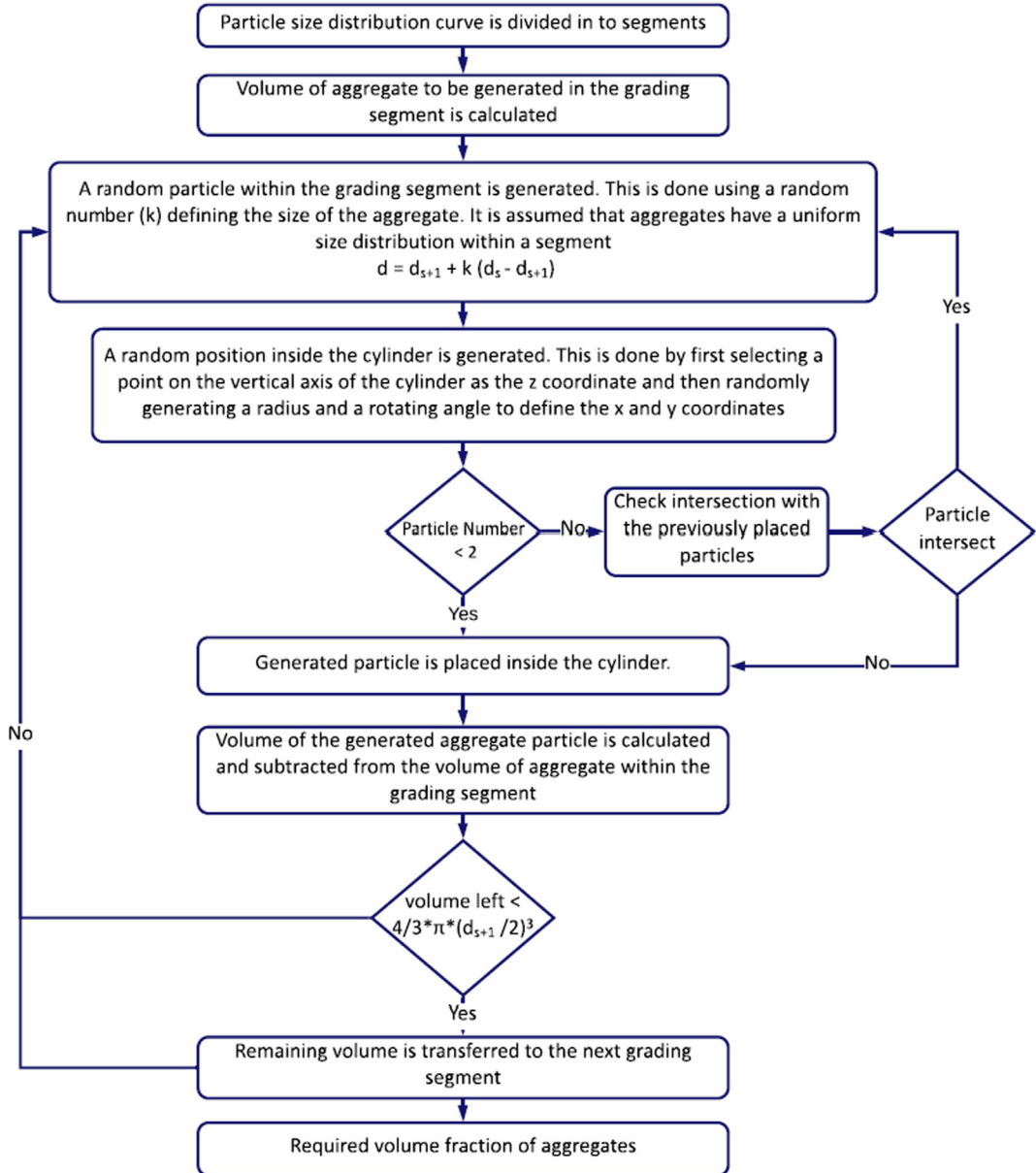


Fig. 6. Flow chart for take and place procedure.

It is important to generate realistic volume fraction of aggregates to represent the concrete behaviour accurately. Generally, concrete has around 40–50% coarse aggregate volume fraction [30]. It is difficult to achieve high volume fractions for polyhedral aggregate particles using take and place method. Various techniques have been used to achieve sufficient aggregate volume fraction such as generation of supplementary particles [41] and shrinking particles from the full Voronoi diagram.

For spherical particles, when the aggregate diameter is smaller, aggregate amount to satisfy a certain weight percentage of that diameter will be very high. Hence in most of the studies [31,55,56] aggregates with diameter less than 4.75 mm are not modelled. It is assumed that the particles less than that diameter are included in the mortar matrix [57].

Take and place method can be recommended as the best method to generate and distribute spherical aggregate particles due to its simplicity. Using take and place method realistic volume fraction for spherical particles can be achieved and with the current computer capacities, generation time will be insignificant. Take and place method can be used to achieve smaller volume fractions up to 30% for polyhedral particles [41]. However, for polyhedral particles, it is difficult to achieve a higher volume fractions using take and place method and hence, for polyhedral particles, aggregate shrinking method [39] can be recommended which can achieve volume fractions up to 67%.

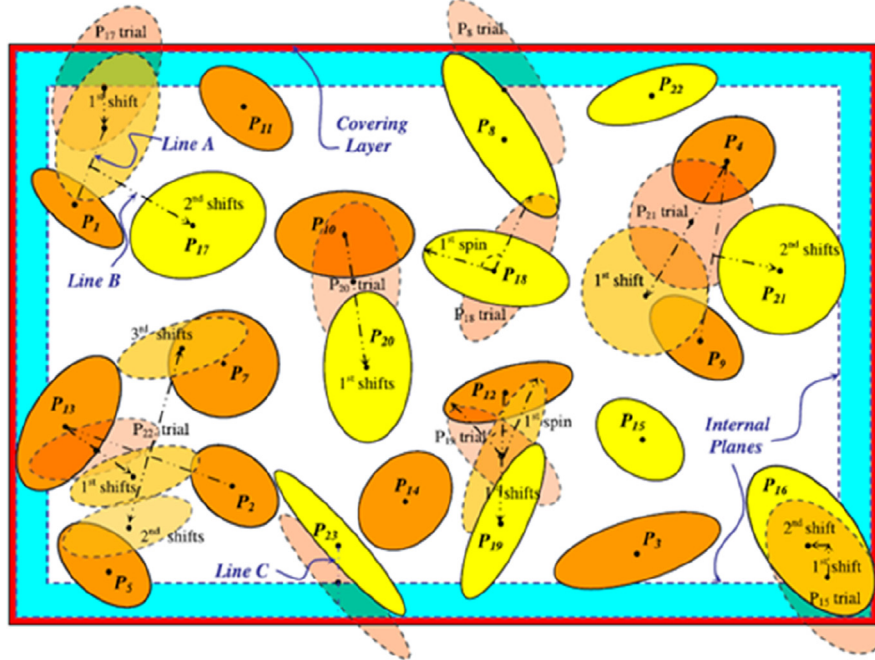


Fig. 7. 2D Representation of Stochastic Heuristic algorithm [53].

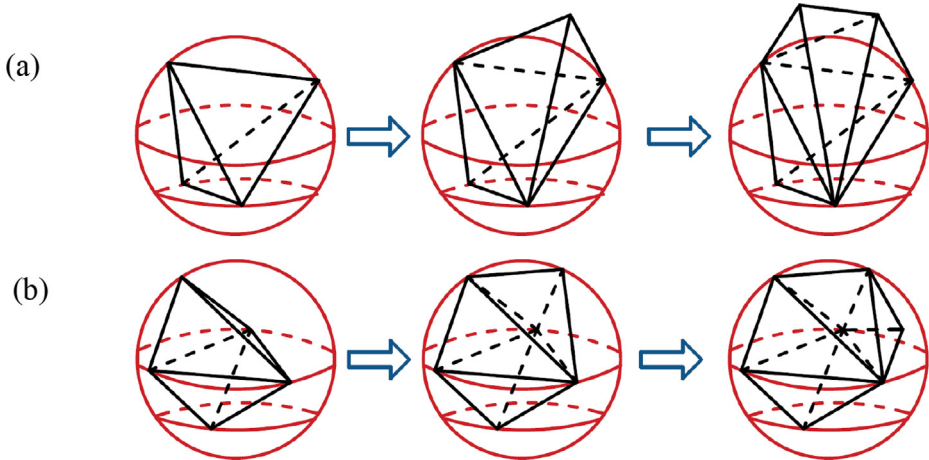


Fig. 8. (a) Aggregate extension starting from a tetrahedral aggregate (b) aggregate extension starting from a hexahedral aggregate [54].

#### 2.2.4. ITZ and mortar geometry generation

Interfacial Transition Zone (ITZ) is an important aspect in mesoscale modelling of concrete because it is widely considered to be the weakest link where fracture initiates. Various methods have been used to represent the ITZ in mesoscale models by researchers. Actual thickness of the ITZ in concrete is around 10–50 µm [58,59]. However, in mesoscale modelling it is not efficient to model elements with such small thickness due to the drastic increase of number of finite elements and hence the computational effort. Hence, feasible thicknesses are used considering the element size in the mesh.

ITZ can be represented using a thin layer of solid finite elements surrounding the aggregate particles [60]. One way to generate this thin layer is by shrinking the aggregate particles. This generates a layer between the aggregate particles and the mortar matrix. This layer is meshed to create the ITZ layer in between the particle and the mortar. However, in this method the negligibly small thickness of ITZ compared with the mesoscale of concrete is not represented realistically. Schrader and Körnke [61] proposed another method to generate volumetric ITZ. In this method, structured grid discretization was applied in the matrix region and bounding boxes were created in the inclusion region with the ITZ. Elements within this bounding box were discretized using an aligned mesh and by element shifting number of elements in ITZ were adjusted.

Another method is to represent the ITZ using zero thickness cohesive elements [62–67]. These zero thickness cohesive elements are inserted in between the aggregates and the mortar phase. In many instances, these zero thickness cohesive elements were found to

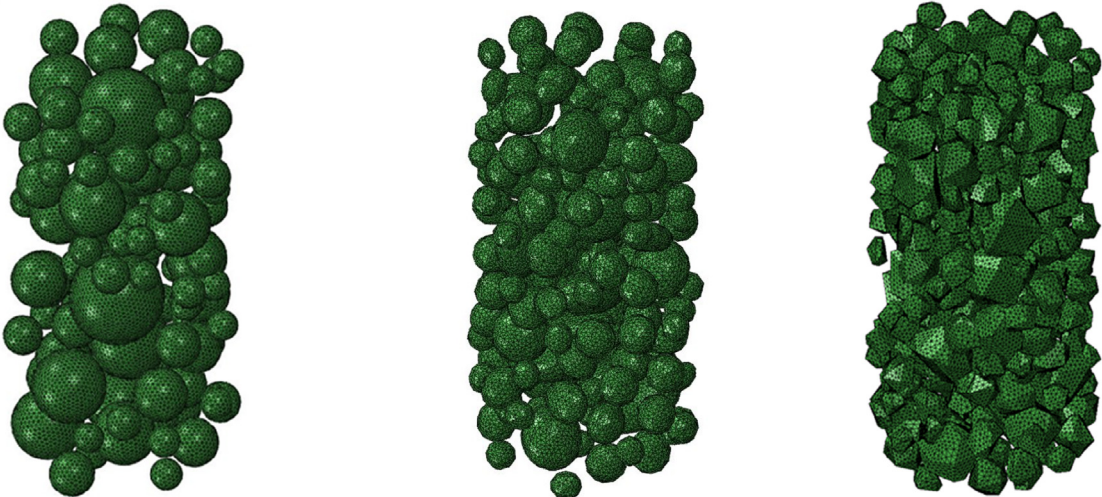


**Fig. 9.** Finite element meshes of different aggregate types.

be representing the ITZ well. However, when compressive forces are applied in the thickness direction in zero thickness elements, element nodes can get cross penetrated which might cause errors in the simulation.

Tu and Lu [68] developed two mesoscale models with ITZ. In one of the models ITZ was modelled using zero thickness cohesive elements and in the other model ITZ was represented using separate finite elements. It was found that the model which used cohesive elements failed to generate a realistic response and the models which represented ITZ using finite elements behaved realistically. In the scenario where, cohesive elements were used to represent ITZ, cross penetration of interface nodes was observed. However, Snozzi et al. [69] used an impenetrability condition to rectify the issue of mesh cross penetration and found that ITZ representation using cohesive elements generated a realistic response.

Mortar phase generation is done by subtracting the volume of the aggregates and from the total volume of the specimen. This can be easily done using most of the finite element analysis software.

#### 2.2.5. Meshing the 3D mesostructure

After generating the geometrical model, it needs to be meshed for analysis. Various techniques for meshing have been applied by researchers. One approach is aligned meshing where the material interfaces would coincide with finite element boundaries [70]. This will generate a clear boundary between the matrix and particles. Aligned meshing has been used by many researchers [36,71–75]. Other approach is to use an unaligned meshing where material interfaces does not coincide with the finite element boundaries. In this approach, finite elements will have material discontinuities inside them.

Developed geometry can be meshed using meshing software and codes. Zhou et al. [41] used a meshing code TetGen [76] which uses Delaunay triangulation to mesh the geometry generated in Matlab. Han et al. [14] used MSC/PATRAN commercial preprocessor to mesh the geometry using 10 node tetrahedral elements. Spherical, ellipsoidal and polyhedral aggregates with aligned meshing which were meshed using Hypermesh [77] are shown in Fig. 9.

Meshing the ITZ is also an important aspect of the mesh generation of the mesoscale model. Since the thickness of the ITZ is significantly lower compared with aggregates, mesh generation will result in issues. If hexahedral or tetrahedral elements of thickness of 10–50  $\mu\text{m}$  are used to mesh the ITZ millions of elements will be generated and that is not a feasible option. Li and Li [23] proposed a method called Aggregate Expansion Method (AEM) to mesh the ITZ with wedge elements with thickness of 50  $\mu\text{m}$ . Generally, ITZ element thickness is taken to be around 0.2–0.8 mm in the mesoscale model [78] which is not accurate in reality.

Cubic meshes, or voxels are used to discretize the concrete volume by projecting a regular mesh into the random aggregate structure as shown in Fig. 10 [79]. Zohdi and Wriggers [70] used an unaligned cubic mesh in the mesoscale model developed. When the cubic meshes are used to model a concrete cylinder, actual shape of the concrete cylinder cannot be obtained due to the curved shape of the cylinder [80]. Also, when spherical particle shape is used, particles cannot be meshed with a smooth particle shape due to the cubic nature of the mesh. Only an approximation of the geometry can be obtained and when smaller mesh sizes are used, the geometry becomes closer to the actual geometry.

Voxel unaligned meshing is mainly used when the mesostructure of the concrete developed using digital image-based approach. It is convenient to represent pixels of the scanned model using a voxel mesh [13]. Voxel meshes are also mainly used to represent the diffusion process inside concrete at mesoscale due to the convenience of identifying the element connectivity due to the regular geometry of the elements [81–83]. Voxel representation of the mesoscale mesh is convenient due to its simplicity but for fracture and damage investigations, it has been found that the voxel mesh does not realistically represent the post peak behavior and the residual strength compared with tetrahedral meshing [79]. Hence, for parameterization models which are used to investigate damage and fracture of concrete, an aligned tetrahedral meshing can be recommended.

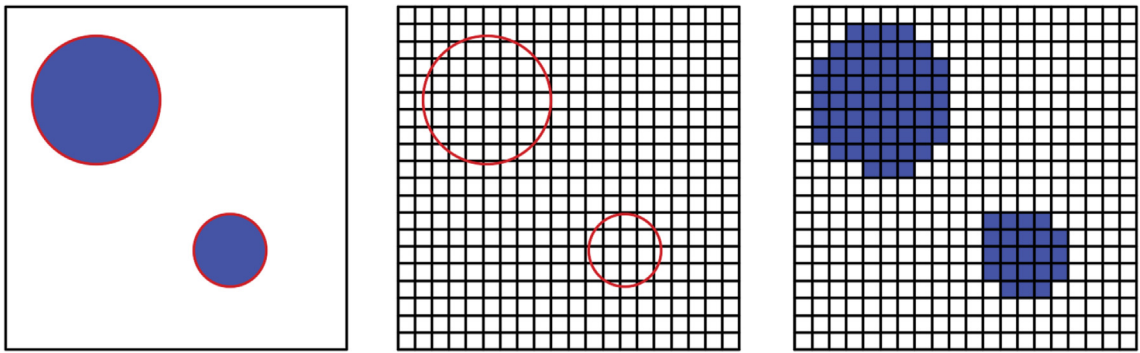


**Fig. 10.** Cross section of a voxel mesh [79].

### 3. Generation of geometry for meso-scale – discrete methods

#### 3.1. Discrete element method

Discrete element method (DEM) is one of the main discrete analysis methods which has been used to model concrete in mesoscale. In this method equilibrium forces and displacements of a set of particles are found using a calculation tracing the particle movements [84]. Geometric shape of these discrete particles is spherical in most instances. Particles with non-spherical shapes can also be used such as ellipsoids and polyhedrons. However, this increases the requirement of computational resources drastically.

Aggregates in the discrete element models can be represented using one particle [16,85–89] or using a cluster of particles [90–94] as shown in Figs. 11 and 12. When one particle is used to represent the aggregates, particles can be generated according to a particle size distribution. When particles are generated, higher compaction should be achieved and particles should not be overlapped.

Mortar is also represented by discrete particles. In this case, the particle size should be smaller compared with the aggregate particle size. When the size of the particle becomes smaller, number of particles and the simulation time increase significantly.

Growing particle method can be used to achieve a higher volume fraction of particles with a good compaction. In this method, aggregate and mortar particles are randomly generated and distributed within the bounds. Particles are grown until they reach their final size from a distribution of points. When these particles are growing, they move around when they come into contact and this process is continued until the total kinetic energy of the assembly reaches zero [88].

It should be noted that the analysis of 3D models in DEM requires higher computational resources compared with the 2D DEM and hence not many 3D models in mesoscale have been analyzed by previous researchers.

#### 3.2. Rigid Body Spring Model

Rigid Body Spring Model (RBSM) was introduced by Kawai [97] where the structure is discretized into rigid sections and these sections are connected using zero size springs distributed in the contact boundaries [16]. Voronoi diagrams are generally used to partition the continuum into rigid bodies.

A 3D Voronoi diagram of the specimen is created using Voronoi cells and these cells represents the aggregates and mortar in mesoscale as shown in Fig. 13. There will be no gaps in between discrete Voronoi cells as in the case of discrete element method.

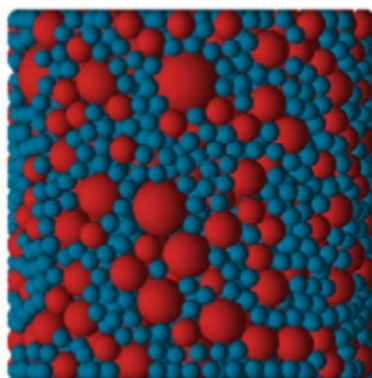


**Fig. 11.** DEM with aggregate represented by a single particle [95].

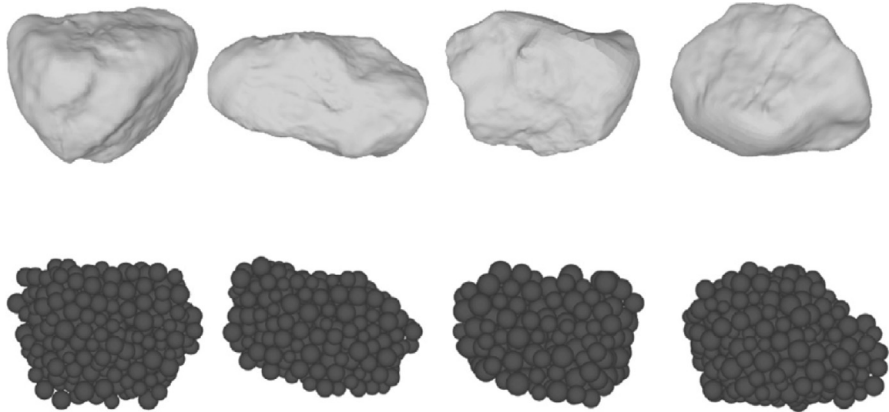


**Fig. 12.** Aggregates represented by cluster of particles [96].

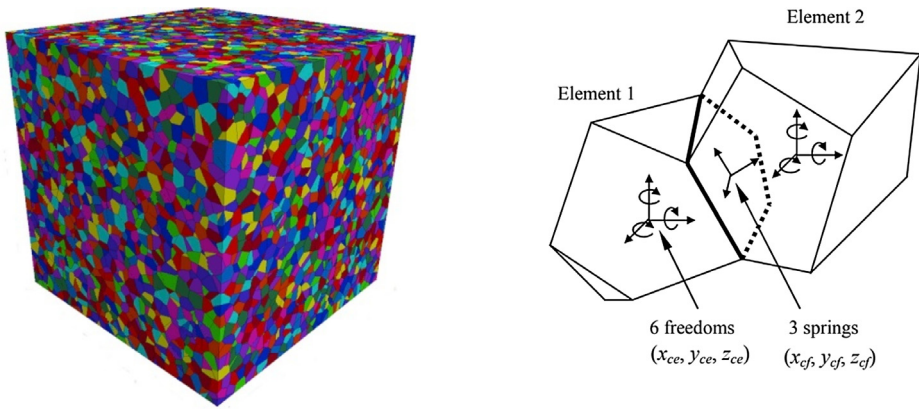


**Fig. 13.** 3D Voronoi diagram [96] and Voronoi cells [98].

### 3.3. Lattice element methods

In lattice models, a continuum is discretized using a set of cells which forms a grid as shown in Fig. 14. Then a cubic core is defined in each of the cells and a random node is generated inside this cubic core. After forming the node array, lattice network can be generated by either using Delaunay triangulation or by simply connecting the nodes of each cells by line elements such as beams, trusses and springs [99]. In contrast to the random method described above, the lattice arrangement can be obtained by a regular lattice where the lengths of the lattice elements are similar [100].

In lattice models, arrangement of the particle structure can be achieved without having to generate complicated shapes like polyhedrons [101]. These lattice structures can have various geometrical arrangements such as triangular lattices, square lattices, random lattices as shown in Fig. 15. In beam lattice models, the connection between nodes can be achieved either using Euler-Bernoulli beams or using Timoshenko beams. If the lattice elements are short and deep, Timoshenko beams should be used [102].

There is another variation of Lattice element method called Lattice Discrete Particle Method. LDPM is a combination of the DEM and the confinement shear lattice model [104–106]. In LDPM, element size in the lattice is not a free parameter as in the traditional lattice methods. Element size is dependent on the aggregate arrangement of the concrete and the lattice nodes are coincident with the centroids of the aggregates [107]. These lattice elements characterize the interaction between aggregates in concrete [16].

## 4. Analysis method and material constitutive models

### 4.1. Continuum methods

After meshing the developed geometry, finite element method can be used to analyze the mesoscale model with suitable material models and properties assigned to the consisting phases. To obtain an accurate response from the finite element analysis, using suitable material parameters and material constitutive models for the consisting phases is vital.

Concrete is a quasi-brittle material of which the yield criterion is dependent on the hydrostatic pressure and has unrecoverable damage and plasticity. The nonlinear behaviour of the concrete is affected by the degradation of elastic modulus as well as the irrecoverable plastic deformations. In mesoscale models, this complex nonlinear behavior of the concrete at macroscale should be

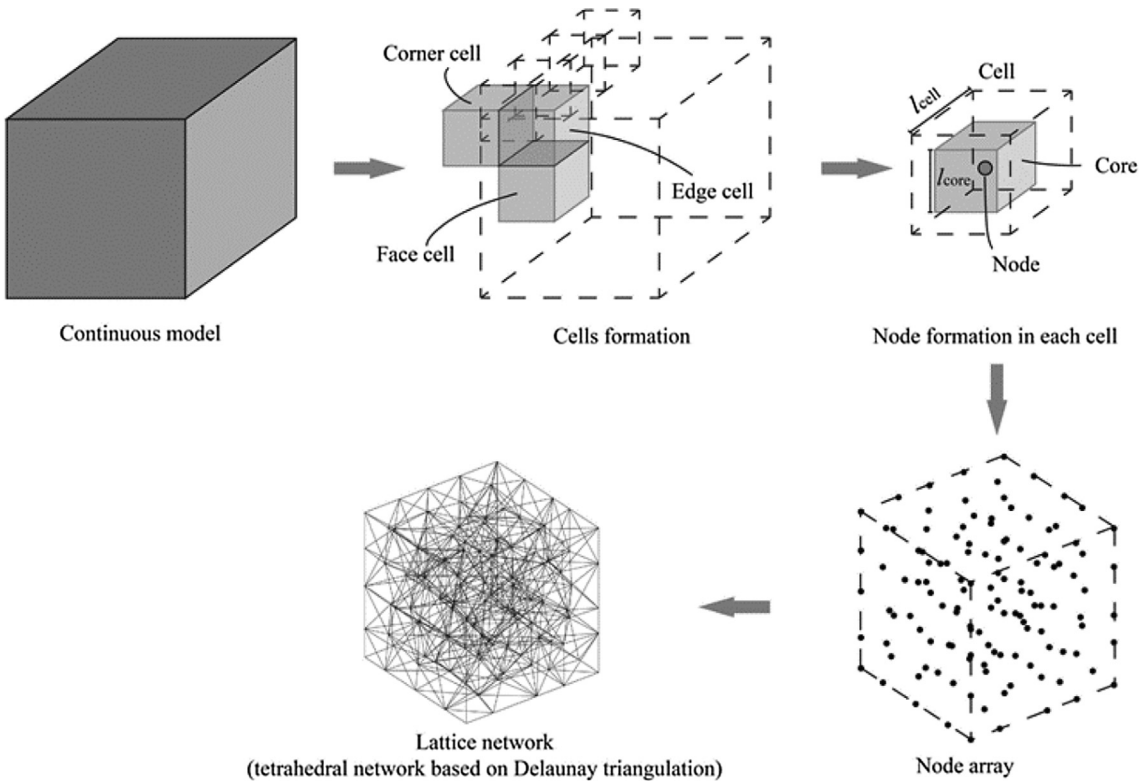


Fig. 14. Process of generating a lattice network.

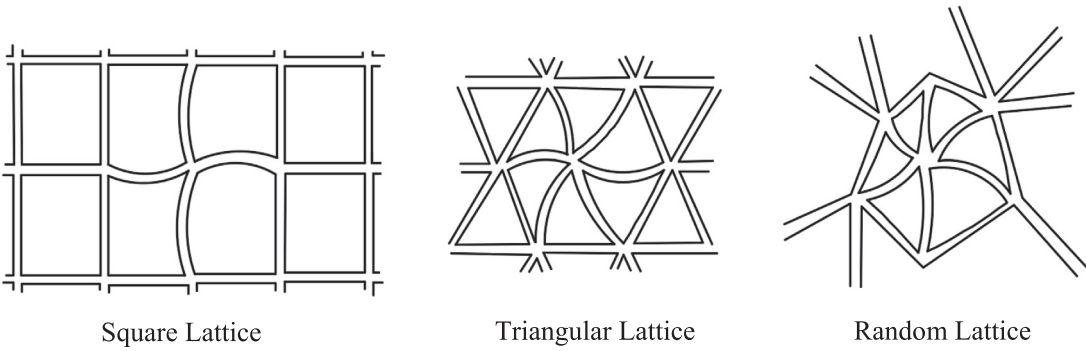


Fig. 15. Geometrical arrangement of lattices [103].

produced using the responses of the individual phases in the mesoscale. For that, accurate material constitutive relations should be assigned to the individual phases in the mesostructure.

Table 2 below gives a summary of the material models used by researchers for the consisting phases of the mesolevel.

Material parameters which are needed for the simulation such as elastic modulus, Poisson ratio, uniaxial tensile strength, uniaxial compressive strength and damage parameters are generally taken using the past literature or conducting experiments [110]. For the three phases in the mesoscale concrete, uniform constant material parameters such as elastic modulus, compressive strength are assigned in most of the mesoscale models. However, to capture the heterogeneity in the meso level, Zhu et al. [117,118] used Weibull probability distribution to vary the material properties of compressive strength, elastic modulus and Poisson's ratio in the mesoscale model. A similar kind of approach was used by Lu and Tu [119] where a probability density function was used to represent non-homogeneous properties in ITZ and aggregates. However, it was found that the non-homogeneity of the mortar phase and ITZ phase has a little impact on the bulk behavior of the mesoscale model of concrete [119]. Therefore, using homogenous properties for phases can be justified for mesoscale modeling.

Description of constitutive relations and the material parameters for the three phases are given in the following sections.

**Table 2**

Summary of the material models used for consisting phases.

Reference	Summary of the material model		
	Mortar matrix	ITZ	Aggregates
Wriggers and Moftah [8]	Isotropic damage model	Not modelled	Linearly elastic
Zhang et al. [39]	Holmquist-Johnson-Cook (HJC) model	Not modelled	Holmquist-Johnson-Cook (HJC) model
Lv et al. [108]	Holmquist-Johnson-Cook (HJC) model	Holmquist-Johnson-Cook (HJC) model	Holmquist-Johnson-Cook (HJC) model
Zhou et al. [41]	K&C Concrete Damage Model	K&C Concrete Damage Model	K&C Concrete Damage Model
Shahbeyk et al. [31]	Plastic damage model proposed by Lee and Fenves [109]	Not modelled	Linearly elastic
Tu and Lu [68]	Concrete Damage Model #71 LS DYNA	Concrete Damage Model #71 LS DYNA	Linearly elastic
Song and Lu [60]	K&C Concrete Damage Model	K&C Concrete Damage Model	Nonlinear plastic
Hao and Hao [44]	MAT_72R3 in LSDYNA	Not Modelled	PSEUDO_TENSOR (Mat_16 in LSDYNA)
Contrafatto et al. [110]	Drucker Prager model	Not Modelled	Drucker Prager model
	Ottosen model		Ottosen model
Unger et al. [111]	plasticity model with isotropic damage model	Cohesive model	Linearly elastic
Huang et al. [26]	Concrete damaged plasticity model (CDPM)	Concrete damaged plasticity model (CDPM)	Linearly elastic
Chen et al. [112]	Concrete damaged plasticity model (CDPM)	Concrete damaged plasticity model (CDPM)	Linearly elastic
Du et al. [113]	Concrete damaged plasticity model (CDPM)	Not Modelled	Linearly elastic
Xu and Chen [114]	Elasto-viscoplastic damage model	Elasto-viscoplastic damage model	Linearly elastic
Tal and Fish [9]	Gurson model	Not Modelled	Linearly elastic
Chen et al. [115]	Concrete damaged plasticity model (CDPM)	Concrete damaged plasticity model (CDPM)	Linearly elastic
Liu et al. [116]	Concrete damaged plasticity model (CDPM)	Concrete damaged plasticity model (CDPM)	Linearly elastic

#### 4.1.1. Constitutive relations for aggregate phase

Most researchers have used a linear elastic material model for aggregates in normal strength concrete under low rate of loadings which can be reasonable because the failure is going through the mortar and the ITZ and aggregate remain in elastic stage [116].

However, for high strength concrete, researchers have stated that aggregate might get crushed and failure surface might go through the aggregate rather going around the ITZ [20,217–221]. Therefore, for high and very-high strength concrete, nonlinear material models shall be used for aggregates. Holmquist-Johnson-Cook (HJC) model has been successfully used to represent the fracture of aggregates in mesoscale concrete models with dynamic loadings [39]. This material model includes a damage model, equivalent strength model and an equation of state to capture the pressure dependency. However, this model is suitable for materials which are subjected to high strain rate loadings [121].

#### 4.1.2. Constitutive relations for mortar phase

Generally, isotropic plasticity model is combined with isotropic or anisotropic damage model to represent the mortar material behaviour [111].

Most of the researchers have used CDPM to represent the behavior of mortar as shown in Table 2. This model uses the yield criterion developed by Lubliner et al. [122] and modified by Lee and Fenves [109]. This uses a non-associated plastic flow based on Drucker-Prager hyperbolic function and also a isotropic damage model. Chen et al. [115] included a Dynamic Increase Factor (DIF) in the CDPM to model the dynamic compressive behavior of concrete.

Most of the researchers [8,117,118,123] have used an isotropic damage model where the stiffness is assumed to degrade linearly according to the Eq. (5).

$$E = (1 - D)E_0 \quad (5)$$

where  $E$  is the elastic modulus of the damaged material and  $E_0$  is the elastic modulus of the undamaged material and  $D$  is the damage parameter. Kim and Abu Al-Rub [124] used a nonlinear isotropic damage model instead of a linear damage model based on the findings of Cicekli et al. [125]. Zhu et al. [117] used two constitutive models for an element subjected to uniaxial tension. One is a brittle isotropic damage model and the other is a ductile isotropic damage model where the softening branch is described using the power function. Shear damage has also been considered in mesoscale models. Zhu et al. [117] included Mohr-Coulomb criterion to identify the shear damage in the meso model. Most of the researchers have used isotropic damage models combined with isotropic plasticity as mentioned above. However, anisotropic damage models [124] have also been used in conjunction with the isotropic plasticity.

#### 4.1.3. Constitutive relations for ITZ phase

ITZ can be considered as a mortar material with increased porosity [116] and hence, most of the researchers have used CDPM to represent the behavior of ITZ as well. Reduced strength and elastic modulus have been used for ITZ in this scenario compared with the mortar phase.

Cohesive contacts and cohesive elements have also been used to model the ITZ successfully [126,127]. Cohesive elements are founded on the basis of cohesive crack models. It is assumed that there is a Fracture Process Zone (FPZ) at the front of crack tip and tractions in normal and two shear direction exist. Traction separation graph is obtained using experiments and damage is incorporated by degrading the stiffness values in normal and shear directions when the separations increase assuming an irreversible progressive damage [128]. However, the separation displacement is difficult to obtain from the experiments and hence, fracture energy is generally used as the fracture initiation criterion [129]. This traction-separation constitutive law for cohesive elements have been widely used in modelling fracture and damage behavior of mesoscale concrete [66].

Mondal et al. [130] found that the elastic modulus of the ITZ is comparable with that of the mortar matrix, using nano indentation. Further, they have shown that there is no clear gradient in material property variation in the ITZ. Generally, material properties of the ITZ is assumed to be constant. In most of the instances, mechanical properties of ITZ is taken as a fraction of the properties of mortar matrix due to the lack of reliable material properties for ITZ. However, nano indentation and nano scratch methods can be used to determine the mechanical properties of ITZ [131].

#### 4.2. Discrete analysis methods

##### 4.2.1. Discrete element method

DEM uses Newton's second law and a contact law to represent the behavior of particles interacting with each other using a time stepping procedure. Resultant forces on the particles are calculated using the interaction of those particles with the neighboring particles which are in contact. To obtain the nonlinear behavior of the concrete, particles should be packed with minimum voids and after packing the particles, first two elements to interact are identified.

Interactions between the particles are modelled using a contact law. Using the constitutive law for the interaction in normal and transverse directions, and equations of motion will be solved [132]. Takada and Hassani [133] illustrated the process of developing and analyzing the discrete element model as shown in Fig. 16.

Interaction between two particles is an important aspect which determines the overall behavior of the mesoscale models. In mesoscale DEM of concrete, a cohesive bond is generally assumed where there are cohesive forces between particles until the breaking criteria is reached. After that bond is broken, a cohesionless contact is assumed between particles. It should be noted that the cohesive interaction is created only at the start of the simulation and when the bond is broken, new bonds are not created.

Azevedo et al. [94] suggested to use the simple brittle Mohr-Coulomb criteria or the extended Mohr-Coulomb criteria as the constitutive law for the interparticle interactions. In the simple Mohr-Coulomb model, the contact is considered to be cracked when the maximum tensile and shear stress values exceed the tensile and shear strength values and the extended Mohr-Coulomb model has a bilinear softening part after the ultimate elastic load as shown in Fig. 17. After the contact is cracked, pure friction will prevail between those particles.

Wang et al. [96] also used a contact model with a linear softening part in the normal direction. However, the stiffnesses of the ascending part and the softening part was considered to be different. The stiffness in the contact model can be taken as a constant value or it can be varied from particle to particle depending on the radii of the particles in contact.

Mohr-Coulomb law without the softening is also used in mesoscale DEM as shown in Fig. 18 [134,135]. In this scenario, after the contact is broken in normal direction, there is no cohesion between particles. When the shear force reaches the limiting value, the contact will be broken but still the frictional component will prevail.

Sinaie [88,89,136] used damage parameters to represent the degradation of the bond depending on the normal and shear displacement in mesoscale concrete models. Two damage parameters  $\delta$  and  $\lambda$  were used to represent the degradation of the strength and the stiffness respectively in normal and shear behavior as shown in Fig. 19.

Tran et al. [137] proposed to use a nonlinear stiffness after reaching the elastic deformation limit to represent the compaction process which is consistent with the triaxial experiments carried out. Total constitutive behavior of their interaction model can be described using the diagram in Fig. 20.

#### 4.3. Rigid body spring model

In this method, concrete specimen is discretized using polyhedrons and the faces of these polyhedrons are connected using springs. Discretized elements are defined as rigid elements and the deformation of the material is represented using the springs [138]. Elastic behaviour of the representing material is obtained by assigning appropriate spring constants. When the model is analyzed, a stiffness matrix is created using the principal of virtual work and the convergence check is carried out using the Newton-Raphson method by checking the unbalanced force and the applied loads.

In contrast to the DEM, this method does not consider the re-contact between the surrounding elements except for the elements where the spring contact is defined at the beginning of the simulation. Stiffness matrix does not need to be updated at every time increment and hence the computational speed is comparatively higher [98].

Mesoscopic behavior of the mortar is simulated using normal and shear springs and the constitutive behaviors are shown in Fig. 21. Springs in the element faces act elastically until the tensile strength criteria or shear strength criteria is reached. In the normal direction, the compression springs are set to always behave elastically. There can be a range of shear strengths as shown in Fig. 21 as the shear strength is considered to be dependent on the condition of the normal spring and the tensile strength. For ITZ a similar constitutive relation is used, and aggregates are assumed to behave elastically without any fracture.

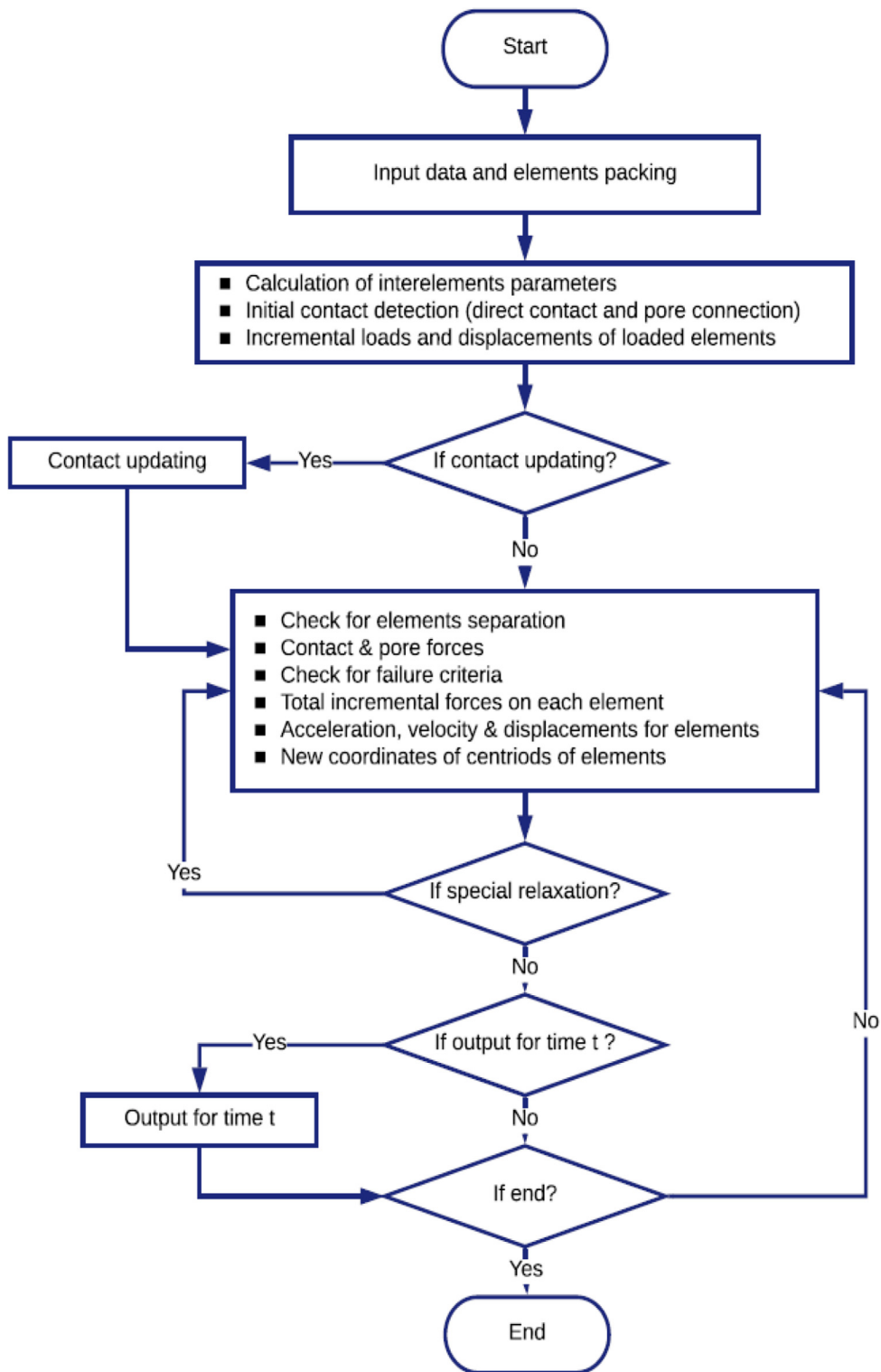


Fig. 16. Discrete Element Method – Flow Chart [133].

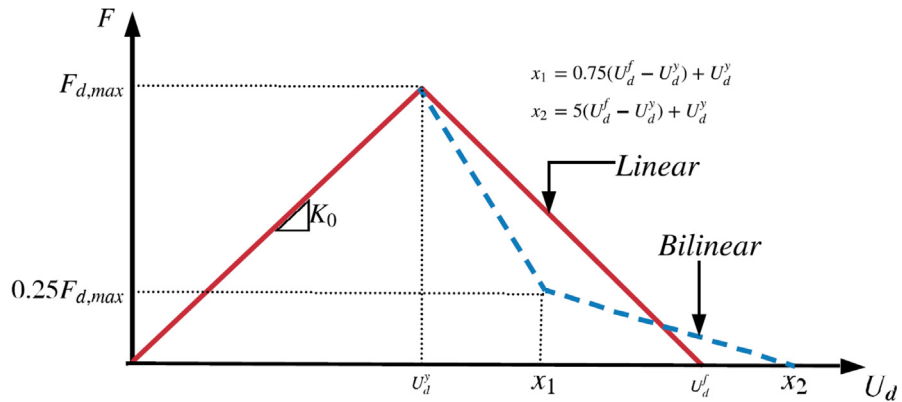


Fig. 17. Simple and extended Mohr - Coulomb model [94].

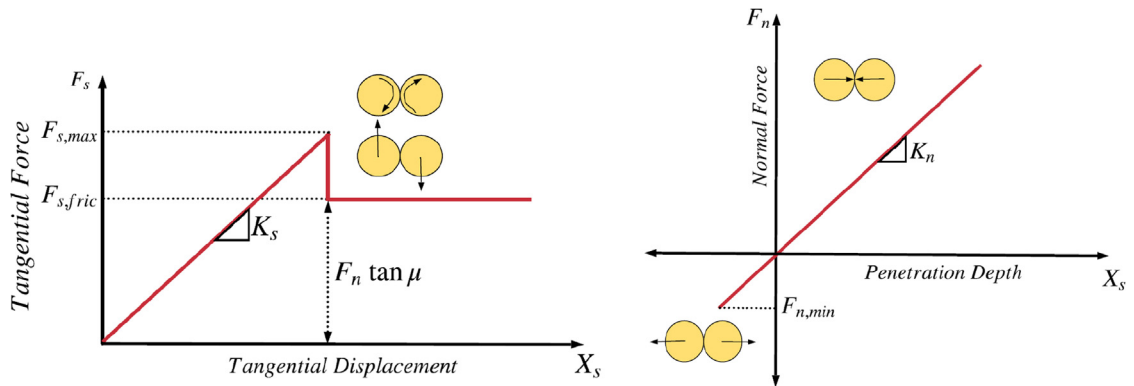


Fig. 18. Tangential and Normal Contact Model without Softening.

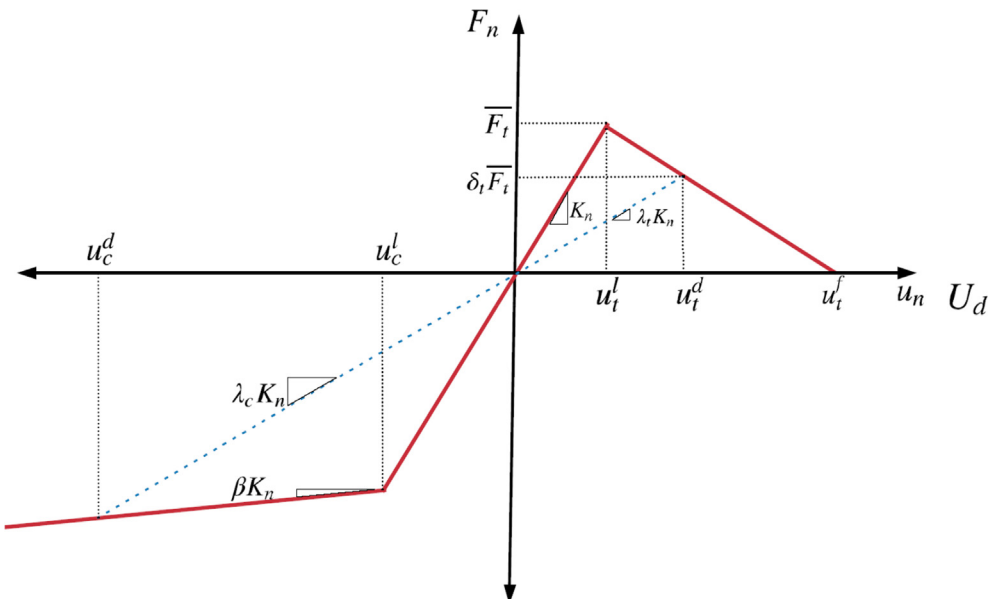


Fig. 19. Normal contact behaviour with damage [89].

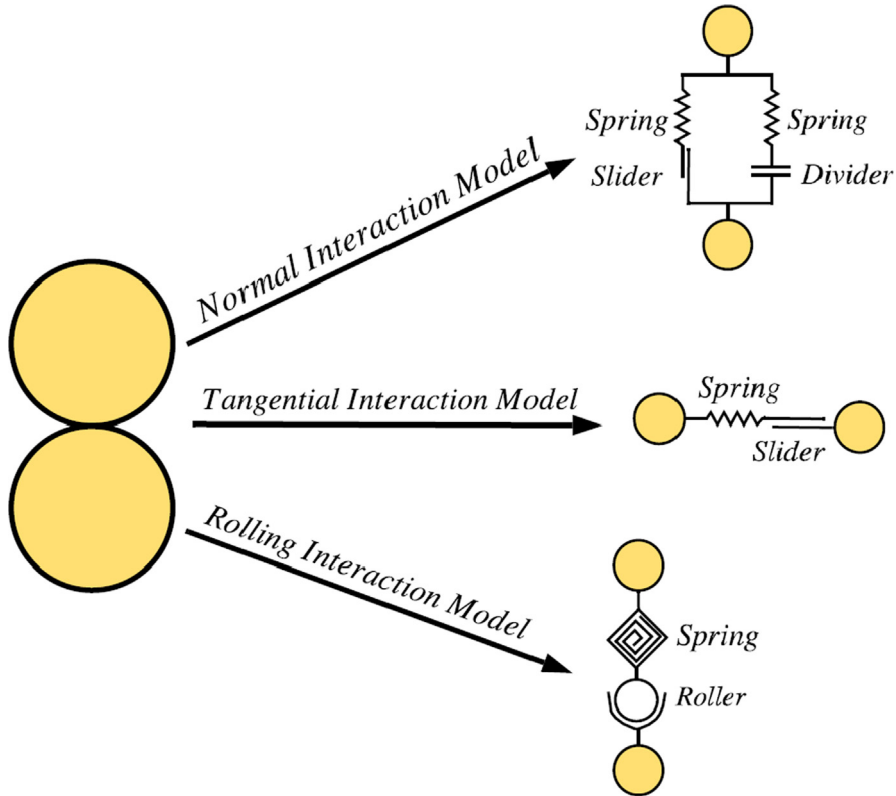


Fig. 20. Rheological Schemes of normal, tangential and rolling interaction.

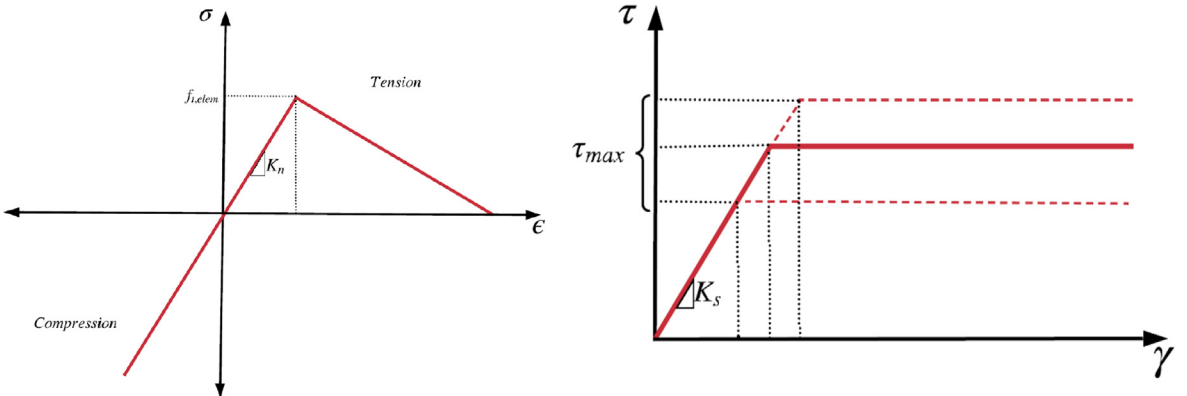


Fig. 21. Constitutive Relations for Normal and Shear Springs.

#### 4.4. Lattice element methods

Lattice element method simulates the mesoscale behavior of concrete by representing the continuum by set of interconnected 1D elements. These elements can be beams, trusses, springs etc. Simple constitutive relations are used to define the failure of these elements and when fracture is happening, element is removed from the mesostructure [139].

It has been found that the fracture behaviour of the model will depend on the fracture law adopted [107] and hence, breaking rule of the element need to represent different behaviors including stretching, bending, and torsion actually happening in the material.

Schlangen and Van Mier [48] used a combination of normal force and bending moment as the fracture criteria for removing the lattice element from the structure using Eq. (6).

$$\sigma_t < \frac{F}{A} + \alpha \frac{(|M_l|, |M_j|)_{max}}{W} \quad (6)$$

where  $\sigma_t$  is the tensile stress in the lattice element. F is the normal force in the element, A is the cross-sectional area of the element,  $M_i$  and  $M_j$  are the bending moments of the nodes i and j of the lattice element, W is the section modulus of the lattice element and  $\alpha$  is a constant depending on the bending failure mode.

Mungule and Raghuprasad [103] used a breaking criterion involving uniaxial tension and a combination of uniaxial tension and bending tension. Strain criterion was used instead of a stress criterion in this scenario as given by Eq. (7).

$$\varepsilon_{element} = \frac{u_2 - u_1}{l} + \frac{d}{2}(r_{2y} - r_{1y}) + \frac{d}{2}(r_{2z} - r_{1z}) \leq \varepsilon^{threshold} \quad (7)$$

where  $u_1$  and  $u_2$  are the displacements of node 1 and node 2 of an element,  $r_{1y}$  and  $r_{2y}$  are the rotations of node 1 and node 2 about y-axis,  $r_{1z}$  and  $r_{2z}$  are the rotations of node 1 and node 2 about z-axis,  $\varepsilon_{element}$  is the strain in the element and  $\varepsilon^{threshold}$  is the limiting strain of the element.

To assign material properties for the lattice elements, a simple procedure can be followed. Lattice can be first projected on to a random aggregate structure or a scanned concrete section and then the end nodes of the lattice elements are checked for their position. If the two nodes in the lattice element lie completely within the mortar, elements are assigned mortar material properties, if the two nodes of the lattice element lie within aggregates, aggregate properties are assigned to the lattice and if one node lies in the aggregate and the other node lies in the mortar, ITZ properties are assigned to that element [140]. Also, some researchers [141] have assigned material properties to the lattice elements using a normal distribution to represent the heterogeneities present in the mesoscale. Generally, linear brittle material properties are assigned to the lattice elements. However, local softening can also be achieved [142].

In LDPM, single lattice elements are used to represent the interaction between aggregates [143]. In this model, midpoints of the concrete aggregates are used as the nodes for the finite element mesh. Both normal and shear stresses characterize the interaction between the aggregate particles. Four aggregates particles whose centers lie in the Delaunay tetrahedral participate to formulate the interactions among the particles. Stresses and strains are defined on every face of the polyhedron which contain the aggregate particles [144].

## 5. Applications, pros and cons of different mesoscale models

### 5.1. Continuum methods - applications

Mesoscale modelling has proven to possess a wide variety of applications in concrete. These applications and the results obtained by researchers are discussed in this section.

Parametric analysis is one main application of the mesoscale models. Using the parametric analysis, impact of critical parameters on the performance of the concrete can be investigated. Kim and Al-Rub [124] developed a 2D mesoscale model using circular aggregates and carried out a parametric analysis by varying critical parameters such as aggregate volume fraction. Concrete model was tested for varying aggregate volume fractions and it was found that when the aggregate volume fraction is increased, cracks in the concrete get localized and the stiffness of concrete increases. Wang et al. [145] developed a 2D mesoscale model using ellipsoidal particle shapes and analyzed the effect of aggregate volume fraction, percentage of pores present in the area and the size of the concrete specimen. It was found that with the increase of size of the concrete specimen, volume fraction of aggregates and percentage of pores in concrete, the peak strength of the concrete reduces. Häfner et al. [38] carried out a similar kind of parametric study about the concrete by changing parameters such as aggregate volume fraction, aggregate stiffness, aggregate shape etc. and predict the effects on concrete properties such as compressive strength and elastic modulus. Wang et al. [146] included voids as spheres into the mesostructure and carried out a parametric study to investigate the effect of voids on the macroscopic concrete behavior. Snozzi et al

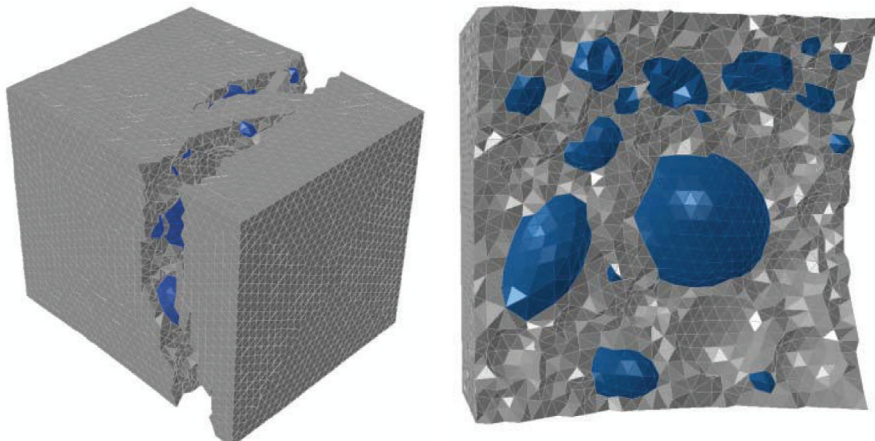


**Fig. 22.** Fracture of concrete under uniaxial tension.

[33] carried out an analysis to investigate the effect of aggregate toughness in concrete under dynamic loading by varying the aggregate toughness. It was found that the macroscopic stress-strain curves for the soft and hard aggregates are similar under loading with high-strain rates and different under the low-strain rate loading.

Concrete fracture and damage propagation behavior is another main researched area using mesoscale models [14,69,147–156]. Fig. 22 shows the fracture behavior obtained from continuum mesoscale modelling for concrete under uniaxial tension. Pedersen et al. [157] investigated the fracture and damage behavior of a 2D mesoscale model with a notch under impact loading. Du et al. [113] investigated the crack propagation behavior of a notched concrete specimen under dynamic loading. From the analysis it was found that the propagation of the cracks depends on the rate of dynamic loading on the specimen. When the loading rate is low, crack propagation is similar to that of a quasi-static test and once the loading rate is increased, cracks show diversification [113]. This fragmentation of concrete under dynamic loading can be explained further by the analytical models proposed by Forquin and Hild [158]. Size effect of concrete is another major area investigated using mesoscale continuum models [159–162]. Snozzi et al. [149] investigated the crack propagation behavior of the concrete with aggregates with various toughness using a cohesive zone model. To represent the cracking in the cement paste, zero thickness cohesive elements can be embedded into the mortar of the mesoscale model [14,69]. Caballero et al. [163–165] used zero thickness interface elements in the potential crack planes in the 3D mesoscale model. In this method cracks can only develop at pre-established cracking paths only. Concrete damage behaviour under high temperature is investigated by Grondin et al. [166] and compared with the experimental results and found to be in good agreement with the experimental results. Corrosion induced cracking of concrete is another aspect investigated by researchers using mesoscale models [147,167,168].

Mesoscale continuum models can be used to obtain fracture parameters. Gangnani et al. [169] found that the increase in aggregate volume fraction will result in an increase in fracture energy of normal strength concrete due to the increase in tortuosity of the crack path by using a mesoscale model. Snozzi et al. [69] investigated how the dissipated fracture energy varies with the strain rate of loading under compression and found that fracture energy dissipation is higher with the increased strain rate. Unger et al. investigated the variation of the macroscopic fracture energy with the specimen size using mesoscale modelling and found that the global fracture energy under uniaxial tension is almost independent of the size of the specimen.

Statistical analysis can be carried out from the mesoscale models when large number of mesoscale models are generated and analyzed. Wang et al. [11] carried out a Monte Carlo simulation using large number of 2D mesoscale models to identify the reliable material parameters and properties. Effect of different aggregate shapes was investigated using circular, elliptical and polygonal shapes. It was found that mean peak stress is marginally higher for circular and elliptical shapes compared with the polygonal aggregates.

Mesoscale models can be used to obtain the macroscopic parameters of the concrete. Du et al. [170] proposed a novel method to obtain the macroscopic behavior using a meso model which is known as Meso Element Equivalent Method (MEEM). This method was aimed at improving the efficiency of meso model calculations. Process of MEEM is represented in Fig. 23. Two-dimensional random aggregate distribution is divided into separate elements and the equivalent mesoscale properties are calculated for each. Using these different properties final model is developed. In this model each element has homogeneous properties inside that element. Voigt parallel method [171] was used to calculate the equivalent material properties.

Wriggers and Moftah [8] analyzed the mesoscale model with compressive loading by displacement control to investigate the nonlinear behavior. Concrete stress-strain curve and damage propagation was obtained as outputs from the mesoscale model. Zhou et al. [41] analyzed a model of a concrete block for uniaxial compression, tension and confined compression under quasi static loading condition and all the stress strain curves had a good match with the experimental results. Feng et al. [172–175] proposed to include randomly distributed microcracks inside the finite element model and using this method, the effective moduli of the microcracked concrete and the fracture propagation and the failure process of the material could be investigated.

Lu and Tu [119] investigated the effect of friction of loading face when the compressive test is carried out. Friction springs were used to simulate the friction behavior of the loading faces of the concrete specimens. It was found that to get a realistic compressive strength of the specimens, friction effects of loading face should be considered. Also, it was found that by considering the loading face friction effects, the failure pattern of the concrete specimens was also changed from an inclined crack mode to a double cone crack

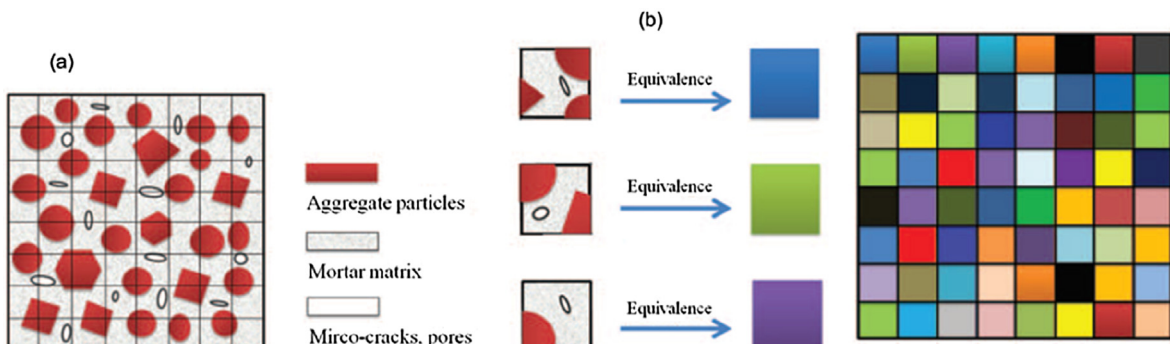


Fig. 23. Process of Meso Element Equivalent Method [170].

pattern which agrees well with the experimental results.

Biaxial loading condition is another type of loading condition that has been applied to the concrete mesoscale model to investigate the behavior of the concrete. Caballero et al. [176] applied seventeen different biaxial loading combination on to the mesoscale models and observed the cracking behavior and the concrete response. It was found that the uniaxial tension and the biaxial tension has the same peak values and the ratio for the biaxial compression to the uniaxial compression kept correct proportion.

Dupray et al. [80] analyzed the mesoscale model under moderate, high and very-high confining loads and obtained the stress-strain curves for the different loading cases and for each loading condition cracking patterns were obtained using the damage behavior. Hao and Hao [44] developed a mesoscale model of a concrete cylinder to simulate the splitting tensile test of concrete and found that the dynamic splitting tensile strength increases when the diameter of the specimens increase.

Effect of ITZ on the macroscale concrete properties have also been investigated using mesoscale models. Zheng et al. [177] used a mesoscale 2D model to develop a numerical method and found that the aggregate area fraction reduces with the increased aggregate diameter. Zheng et al. [178] extended this method using a 3D mesoscale model and investigated the ITZ volume fraction based on the aggregate shape, aggregate volume fraction, ITZ thickness and the aggregate gradation criteria. It was found that the Fuller aggregate gradation has a lower ITZ volume fraction compared with the equal volume fraction (EVF) gradation. Zhou and Hao [78] investigated the behaviour of the concrete when the strength of the ITZ is varied. It was found that the tensile strength of the concrete is increased when the strength of the ITZ is higher. Also, it was found that when the ITZ is thicker, failure starts early, and the tensile strength of the specimen is lower.

Mesoscale models have been used to evaluate the durability aspects such as diffusivity [179–181], alkali silica reaction (ASR), sulfate attack [182] and can be a powerful tool to evaluate the durability of the concrete. Jiang et al. [81] developed a mesoscale model to investigate about the diffusivity of the mortar. It was found that the diffusivity of the mortar reduces when the aggregate fraction in the mesoscale model is increased. Also, diffusivity was calculated by changing the aggregate shape and it was found that the diffusivity was reduced when the aggregate shape is getting closer to the spherical shape. In contrast, Abyaneh et al. [183] found that the diffusivity was reduced when the spherical particles are replaced with the ellipsoidal particles because of the increased tortuosity of the paste. Du et al. [57] developed a similar mesoscale model to investigate about the chloride ingress into the concrete. In this model aggregates are assumed to be impermeable and chloride diffusion is assumed to take place only in mortar and in ITZ. In this study it was found that the aggregate shape and the aggregate distribution has a negligible effect on the chloride ingress of concrete. When the aggregate volume fraction is increased, the overall diffusivity decreased markedly. Li et al. [184] analyzed the permeability variations with respect to mesoscale parameters such as aggregate volume fraction, aggregate shape, thickness and permeability of ITZ etc. using the Monte Carlo simulations. Comby-Peyrot et al. [10] used the developed mesoscale model to simulate the ASR of the concrete. In this study, it was shown that using the mesoscale model, crack patterns due to the alkali-silica reaction can be predicted accurately and the stiffness loss due to the cracks can be predicted accurately [10].

## 5.2. Continuum methods – Pros and Cons

In the continuum method, the geometry of the mesostructure of the concrete can be generated explicitly compared with the discrete models. Aggregates can be realistically modelled according to a particle size distribution curve satisfying the required volume fraction. Hence, continuum methods are more suitable for parametric analysis compared with the discrete models.

Continuum methods have complex constitutive relations to represent the behavior of consisting phases. Number of material parameters to describe the material behavior is higher compared to the discrete models and obtaining accurate material parameters for all three phases is challenging. Also, suitable material models for each consisting phase must be selected and this selection can affect the final results from the simulation.

High computational resources are needed in continuum methods similar to the discrete element models. Mesh sensitivity of the models will affect the results of the simulations and hence a proper size of mesh needs to be selected [2]. However, when the mesh size is too small, the computational resource requirement increases significantly.

In continuum models, fracture path is not generally predefined other than the case where the cohesive elements are preinserted. Hence, a realistic fracture initiation and progression can be obtained compared with the discrete models.

Another main advantage in continuum models is that the material parameters for one stress state can be used to simulate behavior in another stress state and obtain accurate behavior in that loading conditions. For example, Zhou et al. [41] used the same material parameters used when validating the model in compression to achieve accurate results in uniaxial tension as well as confined compression.

## 5.3. Discrete analysis methods

### 5.3.1. Discrete element method - applications

Main application of DEM in mesoscale models is the simulation of fracture behavior of concrete. Rangari et al. [185] developed a 3D discrete element model to investigate the effect of heterogeneity on the compressive strength and the size effect of the concrete specimens and found that there is a strong influence on the meso geometry on the size effect and on compressive strength. Surchorzewski et al. [186] also simulated the size effect in splitting tension and the results were in agreement with the experimental results. Concrete fracture behavior under various loading conditions such as uniaxial compression, uniaxial tension, splitting tension, biaxial loading and triaxial loading have been observed by many researchers using discrete element models [95]. Also, the concrete behavior under dynamic loading has been a main focus area investigated using DEM [90]. Investigation of fracture propagation

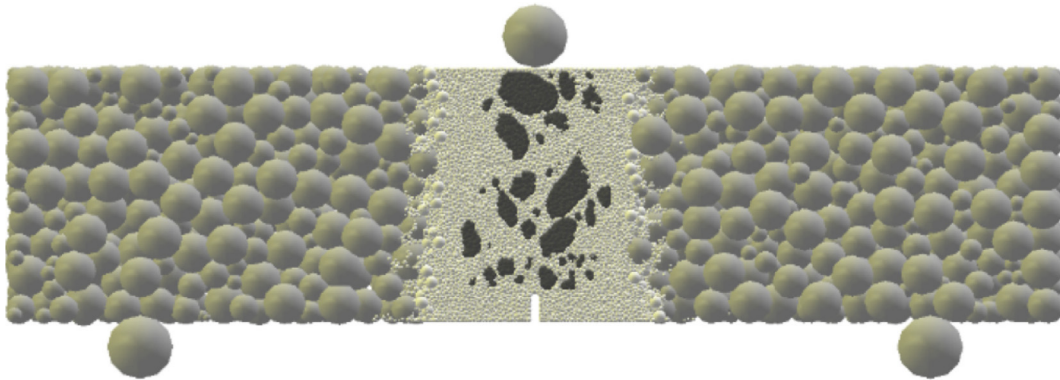


**Fig. 24.** Discrete element model of a notched beam [188].

during bending tests of concrete beams is another application of DEM mesoscale models [187,188]. Wu et al. [4] simulated a drop weight test using a mesoscale dem model of a concrete beam and investigated about the fracture behavior. Nitka and Tejchman [188] analyzed the fracture behavior of a notched beam as shown in Fig. 24 and found that the beam stiffness and strength increased when the microporosity was reduced.

Parametric studies can also be carried out using mesoscale DEM models. Effect of porosity, effect of ITZ on the macro behavior are some of the investigated parameters using these models [46,188]. Wang et al. [96] carried out parametric studies to investigate the effect of aggregate strength and aggregate shape on the strength of concrete. Sinaie et al. [136] carried out a parametric study of strength degradation of concrete due to exposure to the temperature by varying the coefficient of thermal expansion of aggregates and mortar and found that the thermal incompatibility affects the degradation of concrete under elevated temperatures significantly. It should be noted that DEM is less suitable method to carry out the parametric studies compared with the continuum finite element method.

### 5.3.2. Discrete element method – Pros and Cons

DEM uses simple constitutive laws to represent the material behavior compared with the continuum finite element method [188]. Hence, the number of parameters for the constitutive law is smaller and computationally more efficient [189]. However, extensive calibration of the model needs to be done to achieve the accurate response from the model [2]. In this method, local contacts between particles will affect the overall response of the model and the parameters for these local contacts are difficult to obtain using a logical method. Most of the time, these parameters are adjusted to match the overall response of the numerical model to the experimental results. In discrete element models, material parameters for one stress state can be used to simulate behavior in another stress state and obtain accurate behavior in that loading conditions as in the continuum models [185].

DEM is an effective tool to model local phenomena at the mesolevel due to its ability to directly simulate the microstructure using particles [134]. Most of the discrete element models assume aggregates as rigid bodies and hence this is applicable only where transgranular fracture is not happening [185]. However, when the aggregates are modelled as a collection of discrete particles, the transgranular failure can also be modelled.

Discrete element methods require more computational resources compared with the continuum methods [190,191]. Another issue with DEM is the inability to model the geometry of the mesostructure explicitly where in continuum method geometry of the mesostructure can be explicitly modelled. Another issue with DEM simulations is that the ratio of Compressive strength/ Brazilian test strength being lower than the experimental values [96].

### 5.3.3. Rigid body spring model - applications

Fracture analysis concrete can be effectively done using RBSM [84]. Fracture propagation can be modelled by removing the springs or degrading the stiffness values of the springs. In this method, fracture is propagated through interparticle boundaries and hence the fracture pattern might be affected by the arrangement of rigid particles [192]. This can be reduced by using a random mesh design.

Jiradilok et al. [193] investigated about the residual performance of reinforced concrete considering the local damage from the reinforcement corrosion. Reinforcements were modelled using the rigid elements and mesoscale corrosion models were incorporated to RBSM to predict the behavior of corroded reinforced concrete. Hwang and Lim [194] investigated about the fracture due to impact on concrete specimens using a mesoscale RBSM.

### 5.3.4. Rigid body spring model – Pros and Cons

Most of the strengths and weaknesses of the DEM is valid for RBSM as well since it is also a discrete analysis method. Hence, those are not discussed again.

### 5.3.5. Lattice element methods - applications

Investigation of concrete fracture behavior is one of the main applications of lattice element models in mesoscale [195–199]. Karavelić et al. [200] used Timoshenko beam elements embedded with discontinuities to model the failure of concrete. Using the 3D lattice element model, uniaxial tension, hydrostatic tension, uniaxial compression and biaxial compression test simulations were carried out.

Lilliu and van Mier [100] modelled the mesostructure of concrete as a three phase material and investigated the effect of aggregate structure, particle density and bond strength on the fracture behavior. Jirasek and Grassl [55] carried out a mesoscale analysis of concrete using lattice element method to determine the fracture process zone of concrete. Schlangen and Van Mier [48] simulated a single edge notched tensile specimen and found that crack face bridging can be successfully simulated using the mesoscale models. Grassl et al. [201] used a similar lattice model to investigate the size effect of concrete on the fracture process zone. Guo et al. [202] developed a model to investigate the fatigue cracks. Beam and truss elements were used for the lattice element method and it was found that both element types were suitable for fatigue crack modelling. Grassl and Davies [203] investigated about corrosion induced cracking using a mesoscopic lattice element model and concluded that lattice elemet models can realistically represent important aspects in corrosion induced cracking.

Lattice element models have been used to obtain important fracture parameters and their dependence on the mesostructure of concrete. Man and Van Mier [140] calculated the fracture energy using the load-displacement curve obtained from the lattice element simulations and investigated how fracture energy is affected by aggregate shapes and volume fraction.

LDPM is also mainly used to simulate the fracture behavior of concrete in mesoscale [204]. LDPM has found to be realistically simulating most of the loading conditions including quasi static loading, predicting tensile and compressive strength, fracture modelling and size effect of concrete, damage in compression, confined loading conditions etc. [144]. Feng et al. [205] used a mesoscale LDPM to simulate a perforation of a hard projectile into a concrete slab. Cusatis et al. [206] developed a lattice discrete particle meso model of concrete and validated with the experimental results and carried out simulations for unconfined compression, bi-axial behaviour, tri-axial compression, torsional compressive behaviour, cyclic behaviour, tensile fracturing behaviour and tensile splitting test and found that all those loading conditions can be successfully simulated using LDPM. However, It has been found that the fracture behavior simulated using 2D lattice models deviate from the realistic fracture representation [207].

Lattice element models can be used to simulate the transportation phenomenon in cracked concrete [208–210]. Pan et al. [99] investigated about carbonation of concrete using a 3D mesoscale lattice element model and carried out a parametric study to investigate the effects of parameters related to lattice networks on carbonation process. Šavija et al. [211,212] investigated about the chloride ingress into concrete and how the heterogeneity and cracking of the concrete influences the chloride transportation inside the concrete. Creep and shrinkage behavior of concrete is another area which has been investigated using mesoscale lattice models [213,214].

### 5.3.6. Lattice element methods – Pros and Cons

One of the main advantages of lattice element models is its simplicity. Heterogeneities can be conveniently represented by the lattice elements in these models. Failure can be simulated using simple constitutive relations in contrast to the complex material models used in continuum finite element simulations. In these lattice models crack openings can be simulated by breaking the lattice element from the model. However, one drawback of the lattice element method is the inability to model crack closure properly [215].

Most of the lattice model assumes a simple breaking criterion and the element is completely removed from the system when this criterion is satisfied. This can lead to an unrealistic brittle response of the specimen and this can be avoided by modelling the post peak behavior of these elements with a progressive degradation of the stiffness [138].

Fracture pattern is dependent on the element type used in the lattice as well as the orientation of the mesh in the model. Cracks will follow the paths of the mesh and this issue can be solved by using a random lattice in the model [216]. It has been found that the size of the mesh affects the post peak softening behavior of the specimen. Generally, the area under the softening curve should be a constant for the material, but in the lattice element this will change depending on the size of the mesh which is not realistic [200].

One main drawback of lattice models compared with the continuum-based FE models is the difficulty in calculating the effective model parameters [129] because it is difficult to capture lattice parameters using conventional macro scale testing methods. In three-phase lattice models, ITZ has a thickness of one lattice element. However, this thickness values are overestimated because the thickness of ITZ in found to be 10–50  $\mu\text{m}$ . To avoid this issue, either length of the ITZ elements should be reduced or the length of the all elements should be reduced. However, this will increase the number of elements and the computational time and memory as well [51].

## 6. Summary and conclusions

State of the art developments of the different mesoscale modelling methods of concrete considering various methods of generation of the mesostructure are discussed in this paper through past literature. Different methods of geometry formation, particle distribution algorithms, material parameters and material constitutive models, applications, challenges and issues of mesoscale modelling of concrete are discussed with the possible remedies. Following conclusions can be made based on the review.

- Mesoscale modelling techniques can be mainly divided into continuum methods and discrete methods and there are strengths and weaknesses pertaining to each modelling technique and a suitable modelling technique needs to be selected depending on the requirements and available resources

- In continuum modelling, geometry of the mesostructure can be generated using digital image-based approach or using the parameterization approach. Digital image-based approach is suitable for analyzing the actual concrete samples and it can be concluded for parametric studies and statistical analysis of results, parameterization approach is best suited.
- Mesoscale models for continuum models can be analyzed in 2D or in 3D. It can be concluded that 3D models give better representation compared with the 2D models.
- Aggregate particles can be spherical, ellipsoidal or polyhedral in 3D and polyhedral shape can give realistic results compared with other two shapes. Take and place method is the most popular algorithm for particle distribution due to its simplicity. However, when this method cannot achieve a realistic aggregate volume fraction, alternative methods should be used.
- Coupled damage and plasticity models are used widely to represent the mortar in continuum methods. Isotropic plasticity models combined with the isotropic damage models is the most popular combination. Aggregates are represented as a linear elastic material. However, aggregates should also have a coupled damage plasticity behaviour in concrete under dynamic loading or in very high strength concrete since failure goes through aggregate.
- ITZ is represented using cohesive elements or using separate finite element layer. It is not realistic to represent ITZ using separate finite elements due to its very small thickness. When ITZ is represented using cohesive elements, simulation errors can occur due to node cross penetration and a well discretized mesh is needed to avoid these issues. A contact based approached can be used to solve the problem related due to use of cohesive elements.
- Material properties for the material models are taken using past literatures or conducting experiments. However, there is a lack of correct material properties for some material models which represent aggregates and mortar. It is difficult to conduct experiments to obtain properties of ITZ and hence, proportion of mortar material properties are used. However, experimental procedures such as nanoindentation can be used to determine the properties of ITZ.
- In discrete analysis methods, geometry is represented using discrete elements such as spheres in DEM, polyhedral rigid bodies in RBSM, beams and trusses in Lattice element method and in these methods the geometry of the concrete is not explicitly represented
- Simple constitutive relations are used in discrete analysis methods compared to the continuum methods and hence the number of parameters which describes the material behavior is smaller.
- Main application of mesoscale modelling is fracture mechanics of concrete and it can be concluded mesoscale modelling can be successfully used for many other applications such as parametric analysis of concrete, behaviour of concrete under various loading conditions, obtaining macroscopic concrete parameters, durability aspects such as ASR and chloride penetration etc.

#### **Declaration of Competing Interest**

The authors declare that they have no known competing financial interests or personal relationships that could have appeared to influence the work reported in this paper.

#### **Acknowledgement**

P.S.M Thilakarathna would like to thank The University of Melbourne, Australia for providing Melbourne Graduate Research Scholarship Award.

#### **Appendix A. Supplementary material**

Supplementary data to this article can be found online at <https://doi.org/10.1016/j.engfracmech.2020.106974>.

#### **References**

- [1] Nguyen VP, Stroeven M, Sluys LJ. Multiscale failure modeling of concrete: Micromechanical modeling, discontinuous homogenization and parallel computations. *Comput Methods Appl Mech Eng* 2012;201–204:139–56. <https://doi.org/10.1016/J.CMA.2011.09.014>.
- [2] Guo H, Oot ET, Saputra AA, Yang Z, Natarajan S, Ooi EH, et al. A quadtree-polygon-based scaled boundary finite element method for image-based mesoscale fracture modelling in concrete. *Eng Fract Mech* 2019;211:420–41. <https://doi.org/10.1016/j.engfracmech.2019.02.021>.
- [3] Daoud A, Maurel O, Laborde C. 2D mesoscopic modelling of bar-concrete bond. *Eng Struct* 2013;49:696–706. <https://doi.org/10.1016/j.engstruct.2012.11.018>.
- [4] Wu M, Zhang C, Chen Z. Determining the impact behavior of concrete beams through experimental testing and meso-scale simulation: II. Particle element simulation and comparison. *Eng Fract Mech* 2015;135:113–25. <https://doi.org/10.1016/j.engfracmech.2014.12.020>.
- [5] Unger JF, Eckardt S. Multiscale modeling of concrete. *Arch Comput Methods Eng* 2011;18:341–93. <https://doi.org/10.1007/s11831-011-9063-8>.
- [6] Ollivier JP, Maso JC, Bourdette B. Interfacial transition zone in concrete. *Adv Cem Based Mater* 1995;2:30–8. [https://doi.org/10.1016/1065-7355\(95\)90037-3](https://doi.org/10.1016/1065-7355(95)90037-3).
- [7] Zheng JJ, Guo ZQ, Huang XF, Stroeven P, Sluys LJ. ITZ volume fraction in concrete with spheroidal aggregate particles and application: Part II. Prediction of the chloride diffusivity of concrete. *Mag Concr Res* 2011;63:483–91. <https://doi.org/10.1680/macr.2011.63.7.483>.
- [8] Wriggers P, Moftah SO. Mesoscale models for concrete: Homogenisation and damage behaviour. *Finite Elem Anal Des* 2006;42:623–36. <https://doi.org/10.1016/J.FINEL.2005.11.008>.
- [9] Tal D, Fish J. Stochastic multiscale modeling and simulation framework for concrete. *Cem Concr Compos* 2018;90:61–81. <https://doi.org/10.1016/J.CEMCONCOMP.2018.03.016>.
- [10] Comby-Peyrot I, Bernard F, Bouchard P-O, Bay F, Garcia-Diaz E. Development and validation of a 3D computational tool to describe concrete behaviour at mesoscale. Application to the alkali-silica reaction. *Comput Mater Sci* 2009;46:1163–77. <https://doi.org/10.1016/J.COMMATSCL.2009.06.002>.
- [11] Wang XF, Yang ZJ, Yates JR, Jivkov AP, Zhang C. Monte Carlo simulations of mesoscale fracture modelling of concrete with random aggregates and pores. *Constr Build Mater* 2015;75:35–45. <https://doi.org/10.1016/J.CONBUILDMAT.2014.09.069>.

- [12] Yang ZJ, Li BB, Wu JY. X-ray computed tomography images based phase-field modeling of mesoscopic failure in concrete. *Eng Fract Mech* 2019;208:151–70. <https://doi.org/10.1016/j.engfracmech.2019.01.005>.
- [13] Nagai G, Yamada T, Wada A. Three-dimensional nonlinear finite element analysis of the macroscopic compressive failure of concrete materials based on real digital image. In: *Comput Civ Build Eng*. Reston, VA: American Society of Civil Engineers; 2000, p. 449–56. 10.1061/40513(279)59.
- [14] Han W, Eckschlager A, Böhm H. The effects of three-dimensional multi-particle arrangements on the mechanical behavior and damage initiation of particle-reinforced MMCs. *Compos Sci Technol* 2001;61:1581–90. [https://doi.org/10.1016/S0266-3538\(01\)00061-6](https://doi.org/10.1016/S0266-3538(01)00061-6).
- [15] Escoda J, Jeulin D, Willot F, Toulemonde C. Three-dimensional morphological modelling of concrete using multiscale Poisson polyhedra. *J Microsc* 2015;258:31–48. <https://doi.org/10.1111/jmi.12213>.
- [16] Landis EN, Bolander JE. Explicit representation of physical processes in concrete fracture. *J Phys D Appl Phys* 2009;42:214002<https://doi.org/10.1088/0022-3727/42/21/214002>.
- [17] Wang LB, Frost JD, Voyatzis G, Harman TP. Quantification of damage parameters using X-ray tomography images. *Mech Mater* 2003;35:777–90. [https://doi.org/10.1016/S0167-6636\(02\)00206-5](https://doi.org/10.1016/S0167-6636(02)00206-5).
- [18] Ren W, Yang Z, Sharma R, Zhang C, Withers PJ. Two-dimensional X-ray CT image based meso-scale fracture modelling of concrete. *Eng Fract Mech* 2015;133:24–39. <https://doi.org/10.1016/J.ENGFRACMECH.2014.10.016>.
- [19] Huang Y, Yang Z, Ren W, Liu G, Zhang C. 3D meso-scale fracture modelling and validation of concrete based on in-situ X-ray Computed Tomography images using damage plasticity model. *Int J Solids Struct* 2015;67–68:340–52. <https://doi.org/10.1016/J.IJSOLSTR.2015.05.002>.
- [20] Liu T, Qin S, Zou D, Song W, Teng J. Mesoscopic modeling method of concrete based on statistical analysis of CT images. *Constr Build Mater* 2018;192:429–41. <https://doi.org/10.1016/j.conbuildmat.2018.10.136>.
- [21] Yu Q, Liu H, Yang T, Liu H. 3D numerical study on fracture process of concrete with different ITZ properties using X-ray computerized tomography. *Int J Solids Struct* 2018;147:204–22. <https://doi.org/10.1016/j.ijsolstr.2018.05.026>.
- [22] Huang Y, Yan D, Yang Z, Liu G. 2D and 3D homogenization and fracture analysis of concrete based on in-situ X-ray Computed Tomography images and Monte Carlo simulations. *Eng Fract Mech* 2016;163:37–54. <https://doi.org/10.1016/j.engfracmech.2016.06.018>.
- [23] Shuguang L, Qingbin L. Method of meshing ITZ structure in 3D meso-level finite element analysis for concrete. *Finite Elem Anal Des* 2015;93:96–106. <https://doi.org/10.1016/J.FINEL.2014.09.006>.
- [24] Nguyen T, Ghazlan A, Kashani A, Bordas S, Ngo T. 3D meso-scale modelling of foamed concrete based on X-ray Computed Tomography. *Constr Build Mater* 2018;188:583–98. <https://doi.org/10.1016/j.conbuildmat.2018.08.085>.
- [25] Yang Z, Ren W, Sharma R, McDonald S, Mostafavi M, Verityagina Y, et al. In-situ X-ray computed tomography characterisation of 3D fracture evolution and image-based numerical homogenisation of concrete. *Cem Concr Compos* 2017;75:74–83. <https://doi.org/10.1016/j.cemconcomp.2016.10.001>.
- [26] Huang YJ, Yang ZJ, Chen XW, Liu GH. Monte Carlo simulations of meso-scale dynamic compressive behavior of concrete based on X-ray computed tomography images. *Int J Impact Eng* 2016;97:102–15. <https://doi.org/10.1016/J.IJIMPENG.2016.06.009>.
- [27] Mao L, Liu H, Zhu Y, Zhu Z, Guo R, Chiang F, et al. 3D strain mapping of opaque materials using an improved digital volumetric speckle photography technique with X-ray microtomography. *Appl Sci* 2019;9. <https://doi.org/10.3390/app9071418>.
- [28] Xue G, Yilmaz E, Song W, Cao S. Analysis of internal structure behavior of fiber reinforced cement-tailings matrix composites through X-ray computed tomography. *Compos Part B Eng* 2019;175:107091<https://doi.org/10.1016/j.compositesb.2019.107091>.
- [29] Zhang Z, Song X, Liu Y, Wu D, Song C. Three-dimensional mesoscale modelling of concrete composites by using random walking algorithm. *Compos Sci Technol* 2017;149:235–45. <https://doi.org/10.1016/j.compscitech.2017.06.015>.
- [30] Gal E, Ganz A, Hadad L, Kryvoruk R. Development of a concrete unit cell. *Int J Multiscale Comput Eng* 2008;6:499–510. <https://doi.org/10.1615/IntMultCompEng.v6.i5.80>.
- [31] Shahbeyk S, Hosseini M, Yaghoobi M. Mesoscale finite element prediction of concrete failure. *Comput Mater Sci* 2011;50:1973–90. <https://doi.org/10.1016/J.COMMATSCEI.2011.01.044>.
- [32] Häfner S, Eckardt S, Könke C. A geometrical inclusion-matrix model for the finite element analysis of concrete at multiple scales. In: Proc. 16th IKM 2003, Gerlbeck, Hempel, Könke (eds.), Weimar, Ger. June 10–12, 2003.
- [33] Qian Z. Multiscale modeling of fracture processes in cementitious materials (Ph.D Thesis). Technische Universiteit Delft; 2012.
- [34] Mazzucco G, Xotta G, Pomaro B, Salomoni VA, Faleschini F. Elastoplastic-damaged meso-scale modelling of concrete with recycled aggregates. *Compos Part B Eng* 2018;140:145–56. <https://doi.org/10.1016/J.COMPOSITESB.2017.12.018>.
- [35] Zhou Y, Jin H, Wang B. Modeling and mechanical influence of meso-scale concrete considering actual aggregate shapes. *Constr Build Mater* 2019;228. <https://doi.org/10.1016/j.conbuildmat.2019.116785>.
- [36] Wang ZM, Kwan AKH, Chan HC. Mesoscopic study of concrete I: generation of random aggregate structure and finite element mesh. *Comput Struct* 1999;70:533–44. [https://doi.org/10.1016/S0045-7949\(98\)00177-1](https://doi.org/10.1016/S0045-7949(98)00177-1).
- [37] Zhang H, Sheng P, Zhang J, Ji Z. Realistic 3D modeling of concrete composites with randomly distributed aggregates by using aggregate expansion method. *Constr Build Mater* 2019;225:927–40. <https://doi.org/10.1016/j.conbuildmat.2019.07.190>.
- [38] Häfner S, Eckardt S, Luther T, Könke C. Mesoscale modeling of concrete: Geometry and numerics. *Comput Struct* 2006;84:450–61. <https://doi.org/10.1016/J.COMPSTRUCC.2005.10.003>.
- [39] Zhang J, Wang Z, Yang H, Wang Z, Shu X. 3D meso-scale modeling of reinforcement concrete with high volume fraction of randomly distributed aggregates. *Constr Build Mater* 2018;164:350–61. <https://doi.org/10.1016/J.CONBUILDMAT.2017.12.229>.
- [40] Zhang Y, Chen Q, Wang Z, Zhang J, Wang Z, Li Z. 3D mesoscale fracture analysis of concrete under complex loading. *Eng Fract Mech* 2019;220. <https://doi.org/10.1016/j.engfracmech.2019.106646>.
- [41] Zhou R, Song Z, Lu Y. 3D mesoscale finite element modelling of concrete. *Comput Struct* 2017;192:96–113. <https://doi.org/10.1016/J.COMPSTRUCC.2017.07.009>.
- [42] Meddah MS, Zitouni S, Belâabes S. Effect of content and particle size distribution of coarse aggregate on the compressive strength of concrete. *Constr Build Mater* 2010;24:505–12. <https://doi.org/10.1016/J.CONBUILDMAT.2009.10.009>.
- [43] FULLER WB, THOMPSON SE. THE LAWS OF PROPORTIONING CONCRETE. *Trans Am Soc Civ Eng* 1907;LIX:67–143.
- [44] Hao Y, Hao H. Finite element modelling of mesoscale concrete material in dynamic splitting test. *Adv Struct Eng* 2016;19:1027–39. <https://doi.org/10.1177/1369433216630828>.
- [45] Contrafatto L, Cuomo M, Gazzo S. A concrete homogenisation technique at meso-scale level accounting for damaging behaviour of cement paste and aggregates. *Comput Struct* 2016;173:1–18. <https://doi.org/10.1016/J.COMPSTRUCC.2016.05.009>.
- [46] Zhang S, Zhang C, Liao L, Wang C. Numerical study of the effect of ITZ on the failure behaviour of concrete by using particle element modelling. *Constr Build Mater* 2018;170:776–89. <https://doi.org/10.1016/J.CONBUILDMAT.2018.03.040>.
- [47] Rodrigues EA, Manzoli OL, Bitencourt LAG. 3D concurrent multiscale model for crack propagation in concrete. *Comput Methods Appl Mech Eng* 2020;361:112813<https://doi.org/10.1016/j.cma.2019.112813>.
- [48] Schlangen E, van Mier JGM. Simple lattice model for numerical simulation of fracture of concrete materials and structures. *Mater Struct* 1992;25:534–42. <https://doi.org/10.1007/BF02472449>.
- [49] Wang W, Wang J, Kim M-S. An algebraic condition for the separation of two ellipsoids. *Comput Aided Geom Des* 2001;18:531–9. [https://doi.org/10.1016/S0167-8396\(01\)00049-8](https://doi.org/10.1016/S0167-8396(01)00049-8).
- [50] Bailakanavar M, Liu Y, Fish J, Zheng Y. Automated modeling of random inclusion composites. *Eng Comput* 2014;30:609–25. <https://doi.org/10.1007/s00366-012-0310-x>.
- [51] Bazant ZP, Tabbara MR, Kazemi MT, Pijaudier-Cabot G. Random particle model for fracture of aggregate or fiber composites. *J Eng Mech* 1990;116:1686–705. [https://doi.org/10.1061/\(ASCE\)0733-9399\(1990\) 116:8\(1686\)](https://doi.org/10.1061/(ASCE)0733-9399(1990) 116:8(1686).
- [52] Wittmann FH, Roelfstra PE, Sadouki H. Simulation and analysis of composite structures. *Mater Sci Eng* 1985;68:239–48. [https://doi.org/10.1016/0025-2313\(85\)90005-0](https://doi.org/10.1016/0025-2313(85)90005-0).

- 5416(85)90413-6.
- [53] Leite JPB, Slowik V, Mihashi H. Computer simulation of fracture processes of concrete using mesolevel models of lattice structures. *Cem Concr Res* 2004;34:1025–33. <https://doi.org/10.1016/J.CEMCONRES.2003.11.011>.
- [54] Du C, Sun L, Jiang S, Ying Z. Numerical simulation of aggregate shapes of three-dimensional concrete and its applications. *J Aerosp Eng* 2013;26:515–27. [https://doi.org/10.1061/\(ASCE\)AS.1943-5525.0000181](https://doi.org/10.1061/(ASCE)AS.1943-5525.0000181).
- [55] Grassl P, Jirásek M. Meso-scale approach to modelling the fracture process zone of concrete subjected to uniaxial tension. *Int J Solids Struct* 2010;47:957–68. <https://doi.org/10.1016/J.IJSOLSTR.2009.12.010>.
- [56] Zhou XQ, Hao H. Mesoscale modelling and analysis of damage and fragmentation of concrete slab under contact detonation. *Int J Impact Eng* 2009;36:1315–26. <https://doi.org/10.1016/J.IJIMPENG.2009.02.010>.
- [57] Du X, Jin L, Ma G. A meso-scale numerical method for the simulation of chloride diffusivity in concrete. *Finite Elem Anal Des* 2014;85:87–100. <https://doi.org/10.1016/J.FINEL.2014.03.002>.
- [58] Tasong WA, Lynsdale CJ, Cripps JC. Aggregate-cement paste interface: Part I. Influence of aggregate geochemistry. *Cem Concr Res* 1999;29:1019–25. [https://doi.org/10.1016/S0008-8846\(99\)00086-1](https://doi.org/10.1016/S0008-8846(99)00086-1).
- [59] Xia J, Li W, Corr DJ, Shah SP. Effects of interfacial transition zones on the stress-strain behavior of modeled recycled aggregate concrete. *Cem Concr Res* 2013;52:82–99. <https://doi.org/10.1016/j.cemconres.2013.05.004>.
- [60] Song Z, Lu Y. Mesoscopic analysis of concrete under excessively high strain rate compression and implications on interpretation of test data. *Int J Impact Eng* 2012;46:41–55. <https://doi.org/10.1016/J.IJIMPENG.2012.01.010>.
- [61] Schrader K, Könke C. Hybrid computing models for large-scale heterogeneous 3D microstructures. *Int J Multiscale Comput Eng* 2011;9:365–77. <https://doi.org/10.1615/IntJMultCompEng.v9.i4.20>.
- [62] Wu Z, Cui W, Fan L, Liu Q. Mesomechanism of the dynamic tensile fracture and fragmentation behaviour of concrete with heterogeneous mesostructure. *Constr Build Mater* 2019;217:573–91. <https://doi.org/10.1016/j.conbuildmat.2019.05.094>.
- [63] Zhou W, Tang L, Liu X, Ma G, Chen M. Mesoscopic simulation of the dynamic tensile behaviour of concrete based on a rate-dependent cohesive model. *Int J Impact Eng* 2016;95:165–75. <https://doi.org/10.1016/j.ijimpeng.2016.05.003>.
- [64] Trawiński W, Bobiński J, Tejchman J. Two-dimensional simulations of concrete fracture at aggregate level with cohesive elements based on X-ray µCT images. *Eng Fract Mech* 2016;168:204–26. <https://doi.org/10.1016/j.engfracmech.2016.09.012>.
- [65] Xu Y, Zhao S, Jin G, Liang L, Jiang H, Wang X. Explicit dynamic fracture simulation of two-phase materials using a novel meso-structure modelling approach. *Compos Struct* 2019;208:407–17. <https://doi.org/10.1016/j.compstruct.2018.10.029>.
- [66] Trawiński W, Tejchman J, Bobiński J. A three-dimensional meso-scale modelling of concrete fracture, based on cohesive elements and X-ray µCT images. *Eng Fract Mech* 2018;189:27–50. <https://doi.org/10.1016/j.engfracmech.2017.10.003>.
- [67] Tang L, Zhou W, Liu X, Ma G, Chen M. Three-dimensional mesoscopic simulation of the dynamic tensile fracture of concrete. *Eng Fract Mech* 2019;211:269–81. <https://doi.org/10.1016/j.engfracmech.2019.02.015>.
- [68] Tu Z, Lu Y. Mesoscale modelling of concrete for static and dynamic response analysis -Part 1: model development and implementation. *Struct Eng Mech* 2011;37(197–213). <https://doi.org/10.12989/sem.2011.37.2.197>.
- [69] Snozzi L, Gatuingt F, Molinari JF. A meso-mechanical model for concrete under dynamic tensile and compressive loading. *Int J Fract* 2012;178:179–94. <https://doi.org/10.1007/s10704-012-9778-z>.
- [70] Zohdi TI, Wriggers P. Aspects of the computational testing of the mechanical properties of microheterogeneous material samples. *Int J Numer Methods Eng* 2001;50:2573–99. <https://doi.org/10.1002/nme.146>.
- [71] De Schutter G, Taerwe L. Random particle model for concrete based on Delaunay triangulation. *Mater Struct* 1993;26:67–73. <https://doi.org/10.1007/BF02472853>.
- [72] Wittmann F, Sadouki H, Steiger T. Experimental and numerical study of effective properties of Composite materials; 1993. p. 59–82.
- [73] Kwan AKH, Wang ZM, Chan HC. Mesoscopic study of concrete II: nonlinear finite element analysis. *Comput Struct* 1999;70:545–56. [https://doi.org/10.1016/S0045-7949\(98\)00178-3](https://doi.org/10.1016/S0045-7949(98)00178-3).
- [74] Eckardt S, Häfner S, Könke C. Simulation of the fracture behaviour of concrete using continuum damage models at the mesoscale. *Proc. ECCOMAS 2004*, Jyväskylä; 2004.
- [75] Huet C. An integrated approach of concrete micromechanics. *Micromechanics Concr. Cem. Compos.*, Lausanne: Presses Polytechniques et Universitaires Romandes; 1993, p. 117–146.
- [76] Si H. TetGen, a Delaunay-based quality tetrahedral mesh generator. *ACM Trans Math Softw* 2015;41:11.
- [77] Computing A. HyperMesh Reference Manual :- Version 2.1. Altair Computing, Incorporated; 1997.
- [78] Zhou XQ, Hao H. Mesoscale modelling of concrete tensile failure mechanism at high strain rates. *Comput Struct* 2008;86:2013–26. <https://doi.org/10.1016/J.COMPSTRUC.2008.04.013>.
- [79] Montero-Chacón F, Martín-Montín J, Medina F. Mesomechanical characterization of porosity in cementitious composites by means of a voxel-based finite element model. *Comput Mater Sci* 2014;90:157–70. <https://doi.org/10.1016/J.COMMATSCL.2014.03.066>.
- [80] Dupray P, Malecot Y, Daudeville L, Buzaud E. A mesoscopic model for the behaviour of concrete under high confinement. *Int J Numer Anal Methods Geomech* 2009;33:1407–23. <https://doi.org/10.1002/nag.771>.
- [81] Jiang Z, Xi Y, Gu X, Huang Q, Zhang W. Mesoscopic predictions of cement mortar diffusivity by analytical and numerical methods. *J Mater Civ Eng* 2017;29:04016256. [https://doi.org/10.1061/\(ASCE\)MT.1943-5533.0001805](https://doi.org/10.1061/(ASCE)MT.1943-5533.0001805).
- [82] Nilenius F, Larsson F, Lundgren K, Runesson K. Mesoscale modelling of crack-induced diffusivity in concrete. *Comput Mech* 2014;55:359–70. <https://doi.org/10.1007/s00466-014-1105-2>.
- [83] Nilenius F, Larsson F, Lundgren K, Runesson K. Computational homogenization of diffusion in three-phase mesoscale concrete. *Comput Mech* 2014;54:461–72. <https://doi.org/10.1007/s00466-014-0998-0>.
- [84] Bolander JE, Saito S. Fracture analyses using spring networks with random geometry. *Eng Fract Mech* 1998;61:569–91. [https://doi.org/10.1016/S0013-7944\(98\)00069-1](https://doi.org/10.1016/S0013-7944(98)00069-1).
- [85] Asahina D, Landis EN, Bolander JE. Modeling of phase interfaces during pre-critical crack growth in concrete. *Cem Concr Compos* 2011;33:966–77. <https://doi.org/10.1016/J.CEMCONCOMP.2011.01.007>.
- [86] Wang Z, Lin F, Gu X. Numerical simulation of failure process of concrete under compression based on mesoscopic discrete element model. *Tsinghua Sci Technol* 2008;13:19–25. [https://doi.org/10.1016/S1007-0214\(08\)70121-4](https://doi.org/10.1016/S1007-0214(08)70121-4).
- [87] Gu X, Hong L, Wang Z, Lin F. A modified rigid-body-spring concrete model for prediction of initial defects and aggregates distribution effect on behavior of concrete. *Comput Mater Sci* 2013;77:355–65. <https://doi.org/10.1016/J.COMMATSCL.2013.04.050>.
- [88] Sinaie S, Ngo TD, Nguyen VP. A discrete element model of concrete for cyclic loading. *Comput Struct* 2018;196:173–85. <https://doi.org/10.1016/J.COMPSTRUC.2017.11.014>.
- [89] Sinaie S. Application of the discrete element method for the simulation of size effects in concrete samples. *Int J Solids Struct* 2017;108:244–53. <https://doi.org/10.1016/J.IJSOLSTR.2016.12.022>.
- [90] Qin C, Zhang C. Numerical study of dynamic behavior of concrete by meso-scale particle element modeling. *Int J Impact Eng* 2011;38:1011–21. <https://doi.org/10.1016/J.IJIMPENG.2011.07.004>.
- [91] Pan J, Feng YT, Jin F, Xu Y, Sun Q, Zhang C, et al. Meso-scale particle modeling of concrete deterioration caused by alkali-aggregate reaction. *Int J Numer Anal Methods Geomech* 2012;37:n/a-n/a. <https://doi.org/10.1002/nag.2157>.
- [92] Groh U, Konietzky H, Walter K, Herbst M. Damage simulation of brittle heterogeneous materials at the grain size level. *Theor Appl Fract Mech* 2011;55:31–8. <https://doi.org/10.1016/J.TAFMEC.2011.03.001>.
- [93] Grassl P, Rempling R. A damage-plasticity interface approach to the meso-scale modelling of concrete subjected to cyclic compressive loading. *Eng Fract Mech*

- 2008;75:4804–18. <https://doi.org/10.1016/J.ENGFracMech.2008.06.005>.
- [94] Azevedo NM, Lemos JV, de Almeida JR. Influence of aggregate deformation and contact behaviour on discrete particle modelling of fracture of concrete. *Eng Fract Mech* 2008;75:1569–86. <https://doi.org/10.1016/J.ENGFracMech.2007.06.008>.
- [95] Nitka M, Tejchman J. Modelling of concrete behaviour in uniaxial compression and tension with DEM. *Granul Matter* 2015;17:145–64. <https://doi.org/10.1007/s10035-015-0546-4>.
- [96] Wang P, Gao N, Ji K, Stewart L, Arson C. DEM analysis on the role of aggregates on concrete strength. *Comput Geotech* 2019. <https://doi.org/10.1016/j.compgeo.2019.103290>.
- [97] Kawai T. New discrete models and their application to seismic response analysis of structures. *Nucl Eng Des* 1978;48:207–29. [https://doi.org/10.1016/0029-5493\(78\)90217-0](https://doi.org/10.1016/0029-5493(78)90217-0).
- [98] Nagai K, Sato Y, Ueda T. Mesoscopic simulation of failure of mortar and concrete by 3D RBSM. *J Adv Concr Technol* 2005;3:385–402. <https://doi.org/10.3151/jact.3.385>.
- [99] Pan Z, Chen A, Ma R, Wang D, Tian H. Three-dimensional lattice modeling of concrete carbonation at meso-scale based on reconstructed coarse aggregates. *Constr Build Mater* 2018;192:253–71. <https://doi.org/10.1016/j.conbuildmat.2018.10.052>.
- [100] Lilliu G, van Mier JGM. 3D lattice type fracture model for concrete. *Eng Fract Mech* 2003;70:927–41. [https://doi.org/10.1016/S0013-7944\(02\)00158-3](https://doi.org/10.1016/S0013-7944(02)00158-3).
- [101] Man H-K, van Mier JGM. Damage distribution and size effect in numerical concrete from lattice analyses. *Cem Concr Compos* 2011;33:867–80. <https://doi.org/10.1016/j.cemconcomp.2011.01.008>.
- [102] Nikolić M, Karavelić E, Ibrahimbegović A, Miščević P. Lattice element models and their peculiarities. *Arch Comput Methods Eng* 2018;25:753–84. <https://doi.org/10.1007/s11831-017-9210-y>.
- [103] Mungule M, Raguprasad BK. Meso-scale studies in fracture of concrete: A numerical simulation. *Comput Struct* 2011;89:912–20. <https://doi.org/10.1016/J.COMPSTRUCC.2011.02.007>.
- [104] Cusatis G, Bažant ZP, Cedolin L. Confinement-shear lattice model for concrete damage in tension and compression: I. Theory. *J Eng Mech* 2003;129:1439–48. [https://doi.org/10.1061/\(ASCE\)0733-9399\(2003\)129:12\(1439\)](https://doi.org/10.1061/(ASCE)0733-9399(2003)129:12(1439)).
- [105] Cusatis G, Bažant ZP, Cedolin L. Confinement-shear lattice CSL model for fracture propagation in concrete. *Comput Methods Appl Mech Eng* 2006;195:7154–71. <https://doi.org/10.1016/j.cma.2005.04.019>.
- [106] Cusatis G, Bažant ZP, Cedolin L. Confinement-shear lattice model for concrete damage in tension and compression: II. Computation and validation. *J Eng Mech* 2003;129:1449–58. [https://doi.org/10.1061/\(ASCE\)0733-9399\(2003\)129:12\(1449\)](https://doi.org/10.1061/(ASCE)0733-9399(2003)129:12(1449)).
- [107] Pan Z, Ma R, Wang D, Chen A. A review of lattice type model in fracture mechanics: theory, applications, and perspectives. *Eng Fract Mech* 2018;190:382–409. <https://doi.org/10.1016/j.engfracmech.2017.12.037>.
- [108] Lv TH, Chen XW, Chen G. The 3D meso-scale model and numerical tests of split Hopkinson pressure bar of concrete specimen. *Constr Build Mater* 2018;160:744–64. <https://doi.org/10.1016/j.conbuildmat.2017.11.094>.
- [109] Lee J, Fenves GL. Plastic-damage model for cyclic loading of concrete structures. *J Eng Mech* 1998;124:892–900. [https://doi.org/10.1061/\(ASCE\)0733-9399\(1998\)124:8\(892\).](https://doi.org/10.1061/(ASCE)0733-9399(1998)124:8(892).)
- [110] Contrafatto L, Cuomo M, Greco L. Meso-scale simulation of concrete multiaxial behaviour. *Eur J Environ Civ Eng* 2017;21:896–911. <https://doi.org/10.1080/19648189.2016.1182085>.
- [111] Unger JR, Eckardt S, Konke C. A mesoscale model for concrete to simulate mechanical failure. *Comput Concr* 2011;8(401–23). <https://doi.org/10.12989/cac.2011.8.4.401>.
- [112] Chen H, Xu B, Mo YL, Zhou T. Behavior of meso-scale heterogeneous concrete under uniaxial tensile and compressive loadings. *Constr Build Mater* 2018;178:418–31. <https://doi.org/10.1016/j.conbuildmat.2018.05.052>.
- [113] Du X, Jin L, Ma G. Numerical simulation of dynamic tensile-failure of concrete at meso-scale. *Int J Impact Eng* 2014;66:5–17. <https://doi.org/10.1016/j.ijimpeng.2013.12.005>.
- [114] Xu Y, Chen S. A method for modeling the damage behavior of concrete with a three-phase mesostructure. *Constr Build Mater* 2016;102:26–38. <https://doi.org/10.1016/J.CONBUILDMAT.2015.10.151>.
- [115] Chen H, Xu B, Wang J, Zhou T, Nie X, Mo YL. Parametric analysis on compressive strain rate effect of concrete using mesoscale modeling approach. *Constr Build Mater* 2020;246:118375. <https://doi.org/10.1016/j.conbuildmat.2020.118375>.
- [116] Jin L, Wang T, Jiang X, Du X. Size effect in shear failure of RC beams with stirrups: Simulation and formulation. *109573 Eng Struct* 2019;199. <https://doi.org/10.1016/j.engstruct.2019.109573>.
- [117] Zhu WC, Teng JG, Tang CA. Mesomechanical model for concrete. Part I: model development. *Mag Concr Res* 2004;56:313–30. <https://doi.org/10.1680/macr.2004.56.6.313>.
- [118] Zhu WC, Tang CA, Wang SY. Numerical study on the influence of mesomechanical properties on macroscopic fracture of concrete. *Struct Eng Mech* 2005;19(519–33). <https://doi.org/10.12989/sem.2005.19.5.519>.
- [119] Lu Y, Tu Z. Mesoscale modelling of concrete for static and dynamic response analysis -Part 2: numerical investigations. *Struct Eng Mech* 2011;37(215–31). <https://doi.org/10.12989/sem.2011.37.2.215>.
- [120] Shanaka K. Ductility design of very-high strength concrete columns (100 MPa–150 MPa) (Ph.D Thesis). The University of Melbourne; 2016.
- [121] Holmquist TJ, Johnson GR, Cook WH. A computational constitutive model for concrete subjected to large strains, high strain rates and high pressures. In: Murphy MJ, editor. Proc. 14th Int. Symp. Ballist., Quebec, Canada; 1993, p. 591–600.
- [122] Lubliner J, Oliver J, Oller S, Ofiate E. A plastic-damage model for concrete. *Int J Solids Struct* 1989;25:299–326. [https://doi.org/10.1016/0020-7683\(89\)90050-4](https://doi.org/10.1016/0020-7683(89)90050-4).
- [123] Tang X, Zhang C, Shi J. A multiphase mesostructure mechanics approach to the study of the fracture-damage behavior of concrete. *Sci China Ser E Technol Sci* 2008;51:18–24. <https://doi.org/10.1007/s11431-008-6005-2>.
- [124] Kim S-M, Abu Al-Rub RK. Meso-scale computational modeling of the plastic-damage response of cementitious composites. *Cem Concr Res* 2011;41:339–58. <https://doi.org/10.1016/J.CEMCONRES.2010.12.002>.
- [125] Cicekli U, Abu Al-Rub RK. A plasticity and anisotropic damage model for plain concrete. *Int J Plast* 2007;23:1874–900. <https://doi.org/10.1016/J.IJPLAS.2007.03.006>.
- [126] Yilmaz O, Molinari J-F. A mesoscale fracture model for concrete. *Cem Concr Res* 2017;97:84–94. <https://doi.org/10.1016/J.CEMCONRES.2017.03.014>.
- [127] Zhou R, Chen HM, Lu Y. Mesoscale modelling of concrete under high strain rate tension with a rate-dependent cohesive interface approach. *Int J Impact Eng* 2020;139:103500. <https://doi.org/10.1016/j.ijimpeng.2020.103500>.
- [128] Su XT, Yang ZJ, Liu GH. Monte Carlo simulation of complex cohesive fracture in random heterogeneous quasi-brittle materials: A 3D study. *Int J Solids Struct* 2010;47:2336–45. <https://doi.org/10.1016/J.IJSOLSTR.2010.04.031>.
- [129] Wang X, Jivkov AP. Combined numerical-statistical analyses of damage and failure of 2D and 3D mesoscale heterogeneous concrete. *Math Probl Eng* 2015;2015:1–12. <https://doi.org/10.1155/2015/702563>.
- [130] Mondal P, Shah SP, Marks LD. Nanomechanical properties of interfacial transition zone in concrete. *Nanotechnol. Constr.* 3, Berlin, Heidelberg: Springer Berlin Heidelberg; 2009, p. 315–20. 10.1007/978-3-642-00980-8\_42.
- [131] Ngo T, Lee H, Vimonsatit V, Kristombu Baduge K, Mendis P. Properties of matrix, aggregate and interfacial transition zone in very high strength concrete (> 100 MPa) Using Nanoindentation Techniques. *Int. Fed. Struct. Concr.* 5th Int. fib Congr.; 2018.
- [132] Hentz S, Donzé FV, Daudeville L. Discrete element modelling of concrete submitted to dynamic loading at high strain rates. *Comput Struct* 2004;82:2509–24. <https://doi.org/10.1016/J.COMPSTRUCC.2004.05.016>.
- [133] Takada S, Hassani N. Analysis of compression failure of reinforced concrete by the modified distinct element method. *WIT Trans Built Environ* 1970;23. <https://doi.org/10.2495/ERES960341>.
- [134] Suchorzewski J, Tejchman J, Nitka M. Experimental and numerical investigations of concrete behaviour at meso-level during quasi-static splitting tension.

- Theor Appl Fract Mech 2018;96:720–39. <https://doi.org/10.1016/j.tafmec.2017.10.011>.
- [135] Nitka M, Tejchman J. Modelling of concrete fracture at aggregate level using DEM based on X-Ray µCT images of internal structure. In: Proc. 4th Int. Conf. Part. Methods - Fundam. Appl. Part. 2015, International Center for Numerical Methods in Engineering; 2015, p. 343–54. 10.1016/j.englfracmech.2015.08.010.
- [136] Sinaia S, Heidarpour A, Zhao XL. A micro-mechanical parametric study on the strength degradation of concrete due to temperature exposure using the discrete element method. Int J Solids Struct 2016;88–89:165–77. <https://doi.org/10.1016/J.IJSOLSTR.2016.03.009>.
- [137] Tran VT, Donzé FV, Marin P. A discrete element model of concrete under high triaxial loading. Cem. Concr. Compos. 2011;33:936–48. <https://doi.org/10.1016/j.cemconcomp.2011.01.003>.
- [138] Gu X, Jia J, Wang Z, Hong L, Lin F. Determination of mechanical parameters for elements in meso-mechanical models of concrete. Front Struct Civ Eng 2013;7:391–401. <https://doi.org/10.1007/s11709-013-0225-7>.
- [139] Schlangen E, Garboczi EJ. Fracture simulations of concrete using lattice models: Computational aspects. Eng Fract Mech 1997;57:319–32. [https://doi.org/10.1016/S0013-7944\(97\)00010-6](https://doi.org/10.1016/S0013-7944(97)00010-6).
- [140] Man H-K, Mier JGM. Size effect on strength and fracture energy for numerical concrete with realistic aggregate shapes. Int J Fract 2008;154:61–72. <https://doi.org/10.1007/s10704-008-9270-y>.
- [141] Modelization of fracture in disordered systems. Stat Model Fract Disord Media 1990; 159–188. 10.1016/B978-0-444-88551-7.50016-1.
- [142] Qian Z, Schlangen E, Ye G, van Breugel K. 3D lattice fracture model: theory and computer implementation. Key Eng Mater 2010;452–453:69–72. <https://doi.org/10.4028/www.scientific.net/KEM.452-453.69>.
- [143] Zubelewicz A, Bažant ZP. Interface element modeling of fracture in aggregate composites. J Eng Mech 1987;113:1619–30. [https://doi.org/10.1061/\(ASCE\)0733-9399\(1987\)113:11\(1619\)](https://doi.org/10.1061/(ASCE)0733-9399(1987)113:11(1619)).
- [144] Cusatis G, Pelessone D, Mencarelli A. Lattice Discrete Particle Model (LDPM) for failure behavior of concrete. I: Theory. Cem Concr Compos 2011;33:881–90. <https://doi.org/10.1016/J.CEMCONCOMP.2011.02.011>.
- [145] Wang X, Yang Z, Jivkov AP. Monte Carlo simulations of mesoscale fracture of concrete with random aggregates and pores: a size effect study. Constr Build Mater 2015;80:262–72. <https://doi.org/10.1016/J.CONBUILDMAT.2015.02.002>.
- [146] Wang X, Zhang M, Jivkov AP. Computational technology for analysis of 3D meso-structure effects on damage and failure of concrete. Int J Solids Struct 2015;80:310–33. <https://doi.org/10.1016/j.ijsolstr.2015.11.018>.
- [147] Du X, Jin L. Meso-scale numerical investigation on cracking of cover concrete induced by corrosion of reinforcing steel. Eng Fail Anal 2014;39:21–33. <https://doi.org/10.1016/j.engfailanal.2014.01.011>.
- [148] Jin L, Hao H, Zhang R, Du X. Determination of the effect of elevated temperatures on dynamic compressive properties of heterogeneous concrete: A meso-scale numerical study. Constr Build Mater 2018;188:685–94. <https://doi.org/10.1016/j.conbuildmat.2018.08.090>.
- [149] Snozzi L, Caballero A, Molinari JF. Influence of the meso-structure in dynamic fracture simulation of concrete under tensile loading. Cem Concr Res 2011;41:1130–42. <https://doi.org/10.1016/J.CEMCONRES.2011.06.016>.
- [150] Nguyen D, Lawrence C, La Borderie C, Matallah M, Nahas G. A mesoscopic model for a better understanding of the transition from diffuse damage to localized damage. Eur J Environ Civ Eng 2010;14:751–76. <https://doi.org/10.1080/19648189.2010.9693261>.
- [151] Teng JG, Zhu WC, Tang CA. Mesomechanical model for concrete. Part II: applications. Mag Concr Res 2004;56:331–45. <https://doi.org/10.1680/macr.2004.56.6.331>.
- [152] Leite JPB, Slowik V, Apel J. Computational model of mesoscopic structure of concrete for simulation of fracture processes. Comput Struct 2007;85:1293–303. <https://doi.org/10.1016/J.COMPSTRU.2006.08.086>.
- [153] Xu Z, Hao H, Li HN. Mesoscale modelling of fibre reinforced concrete material under compressive impact loading. Constr Build Mater 2012;26:274–88. <https://doi.org/10.1016/J.CONBUILDMAT.2011.06.022>.
- [154] Pedersen RR, Simone A, Sluys LJ. Mesoscopic modeling and simulation of the dynamic tensile behavior of concrete. Cem Concr Res 2013;50:74–87. <https://doi.org/10.1016/J.CEMCONRES.2013.03.021>.
- [155] Congro M, Sanchez ECM, Roehl D, Marangon E. Fracture modeling of fiber reinforced concrete in a multiscale approach. Compos Part B Eng 2019;174:106958. <https://doi.org/10.1016/J.COMPOSITESB.2019.106958>.
- [156] Chaudhuri P. Multi-scale modeling of fracture in concrete composites. Compos Part B Eng 2013;47:162–72. <https://doi.org/10.1016/J.COMPOSITESB.2012.10.021>.
- [157] Pedersen RR, Simone A, Stroeven M, Sluys LJ. Mesoscopic modelling of concrete under impact. Proc. Fram. Catania; 2007.
- [158] Forquin P, Hild F. A Probabilistic Damage Model of the Dynamic Fragmentation Process in Brittle Materials. vol. 44. 2010. 10.1016/S0065-2156(10)44001-6.
- [159] Zhou R, Chen HM. Mesoscopic investigation of size effect in notched concrete beams: The role of fracture process zone. Eng Fract Mech 2019;212:136–52. <https://doi.org/10.1016/j.englfracmech.2019.03.028>.
- [160] Jin L, Yu W, Du X, Yang W. Dynamic size effect of concrete under tension: A numerical study. Int J Impact Eng 2019;132. <https://doi.org/10.1016/j.ijimpeng.2019.103318>.
- [161] Jin L, Yu W, Du X, Zhang S, Li D. Meso-scale modelling of the size effect on dynamic compressive failure of concrete under different strain rates. Int J Impact Eng 2019;125:1–12. <https://doi.org/10.1016/j.ijimpeng.2018.10.011>.
- [162] Jin L, Yu W, Du X, Yang W. Mesoscopic numerical simulation of dynamic size effect on the splitting-tensile strength of concrete. Eng Fract Mech 2019;209:317–32. <https://doi.org/10.1016/j.englfracmech.2019.01.035>.
- [163] Caballero A, López CM, Carol I. 3D meso-structural analysis of concrete specimens under uniaxial tension. Comput Methods Appl Mech Eng 2006;195:7182–95. <https://doi.org/10.1016/J.CMA.2005.05.052>.
- [164] López CM, Carol I, Aguado A. Meso-structural study of concrete fracture using interface elements. II: compression, biaxial and Brazilian test. Mater Struct 2008;41:1601–20. <https://doi.org/10.1617/s11527-007-9312-3>.
- [165] López CM, Carol I, Aguado A. Meso-structural study of concrete fracture using interface elements. I: numerical model and tensile behavior. Mater Struct 2008;41:583–99. <https://doi.org/10.1617/s11527-007-9314-1>.
- [166] Grondin F, Dumontet H, Ben Hamida A, Mounajed G, Boussa H. Multi-scales modelling for the behaviour of damaged concrete. Cem Concr Res 2007;37:1453–62. <https://doi.org/10.1016/J.CEMCONRES.2007.05.012>.
- [167] Xi X, Yang S, Li CQ, Cai M, Hu X, Shipton ZK. Meso-scale mixed-mode fracture modelling of reinforced concrete structures subjected to non-uniform corrosion. Eng Fract Mech 2018;199:114–30. <https://doi.org/10.1016/j.englfracmech.2018.05.036>.
- [168] Xi X, Yang S, Li CQ. A non-uniform corrosion model and meso-scale fracture modelling of concrete. Cem Concr Res 2018;108:87–102. <https://doi.org/10.1016/j.cemconres.2018.03.009>.
- [169] Gangnani A, Saliba J, La Borderie C, Morel S. Modeling of the quasibrittle fracture of concrete at meso-scale: Effect of classes of aggregates on global and local behavior. Cem Concr Res 2016;89:35–44. <https://doi.org/10.1016/J.CEMCONRES.2016.07.010>.
- [170] Du X, Jin L, Ma G. Meso-element equivalent method for the simulation of macro mechanical properties of concrete. Int J Damage Mech 2013;22:617–42. <https://doi.org/10.1177/1056789512457096>.
- [171] Voigt W. Ueber die Beziehung zwischen den beiden Elastizitätsconstanten isotroper Körper. Ann Phys 1889;274:573–87. <https://doi.org/10.1002/andp.18892741206>.
- [172] Feng X-Q, Yu S-W. Damage micromechanics for constitutive relations and failure of microcracked quasi-brittle materials. Int J Damage Mech 2010;19:911–48. <https://doi.org/10.1177/1056789509359662>.
- [173] Feng XQ, Qin QH, Yu SW. Quasi-micromechanical damage model for brittle solids with interacting microcracks. Mech Mater 2004;36:261–73. [https://doi.org/10.1016/S0167-6636\(03\)00021-8](https://doi.org/10.1016/S0167-6636(03)00021-8).
- [174] Feng XQ, Li JY, Yu SW. A simple method for calculating interaction of numerous microcracks and its applications. Int J Solids Struct 2003;40:447–64. [https://doi.org/10.1016/S0020-7683\(02\)00519-X](https://doi.org/10.1016/S0020-7683(02)00519-X).
- [175] Feng XQ. On estimation methods for effective moduli of microcracked solids. Arch Appl Mech 2001;71:537–48. <https://doi.org/10.1007/s004190100161>.

- [176] Caballero A, Carol I, López CM. 3D meso-mechanical analysis of concrete specimens under biaxial loading. *Fatigue Fract Eng Mater Struct* 2007;30:877–86. <https://doi.org/10.1111/j.1460-2695.2007.01161.x>.
- [177] Zheng JJ, Xiong FF, Wu ZM, Jin WL. A numerical algorithm for the ITZ area fraction in concrete with elliptical aggregate particles. *Mag Concr Res* 2009;61:109–17. <https://doi.org/10.1680/macr.2007.00123>.
- [178] Bentz D, Hwang JTG, Hagwood C, Garboczi EJ, Snyder K, Buenfeld N, et al. Interfacial Zone Percolation in Concrete: Effects of Interfacial Zone Thickness and Aggregate Shape. vol. 370. 1994. 10.1557/PROC-370-437.
- [179] Xu J, Li F. A meso-scale model for analyzing the chloride diffusion of concrete subjected to external stress. *Constr Build Mater* 2017;130:11–21. <https://doi.org/10.1016/j.conbuildmat.2016.11.054>.
- [180] Benkemoun N, Hammoud MN, Amiri O. A meso-macro numerical approach for crack-induced diffusivity evolution in concrete 2017. 10.1016/j.conbuildmat.2017.02.146.
- [181] Abyaneh SD, Wong HS, Buenfeld NR. Simulating the effect of microcracks on the diffusivity and permeability of concrete using a three-dimensional model. *Comput Mater Sci* 2016;119:130–43. <https://doi.org/10.1016/j.commatsci.2016.03.047>.
- [182] Idiart AE, López CM, Carol I. Chemo-mechanical analysis of concrete cracking and degradation due to external sulfate attack: A meso-scale model. *Cem Concr Compos* 2011;33:411–23. <https://doi.org/10.1016/j.cemconcomp.2010.12.001>.
- [183] Dehghanpoor Abyaneh S, Wong HS, Buenfeld NR. Modelling the diffusivity of mortar and concrete using a three-dimensional mesostructure with several aggregate shapes. *Comput Mater Sci* 2013;78:63–73. <https://doi.org/10.1016/j.commatsci.2013.05.024>.
- [184] Li X, Xu Y, Chen S. Computational homogenization of effective permeability in three-phase mesoscale concrete. *Constr Build Mater* 2016;121:100–11. <https://doi.org/10.1016/j.CONBUILDMAT.2016.05.141>.
- [185] Rangari S, Murali K, Deb A. Effect of meso-structure on strength and size effect in concrete under compression. *Eng Fract Mech* 2018;195:162–85. <https://doi.org/10.1016/j.engfracmech.2018.04.006>.
- [186] Suchorzewski J, Tejchman J, Nitka M, Bobiński J. Meso-scale analyses of size effect in brittle materials using DEM. *Granul Matter* 2019; 21. 10.1007/s10035-018-0862-6.
- [187] Eliáš J, Vořechovský M, Skoček J, Bažant ZP. Stochastic discrete meso-scale simulations of concrete fracture: Comparison to experimental data. *Eng Fract Mech* 2015;135:1–16. <https://doi.org/10.1016/j.engfracmech.2015.01.004>.
- [188] Nitka M, Tejchman J. A three-dimensional meso-scale approach to concrete fracture based on combined DEM with X-ray µCT images. *Cem Concr Res* 2018;107:11–29. <https://doi.org/10.1016/j.cemconres.2018.02.006>.
- [189] Rodrigues EA, Manzoli OL, Bitencourt Jr. LAG, Bittencourt TN. 2D mesoscale model for concrete based on the use of interface element with a high aspect ratio. *Int J Solids Struct* 2016;94–95:112–24. <https://doi.org/10.1016/J.IJSOLSTR.2016.05.004>.
- [190] Skarzyński Nitka M, Tejchman J. Modelling of concrete fracture at aggregate level using FEM and DEM based on X-ray µCT images of internal structure. *Eng Fract Mech* 2015;147:13–35. <https://doi.org/10.1016/j.engfracmech.2015.08.010>.
- [191] Saksala T. Numerical modelling of concrete fracture processes under dynamic loading: Meso-mechanical approach based on embedded discontinuity finite elements. *Eng Fract Mech* 2018;201:282–97. <https://doi.org/10.1016/j.engfracmech.2018.07.019>.
- [192] Nagai K, Sato Y, Ueda T, Kakuta Y. Numerical simulation of fracture process of plain concrete by rigid body spring method. *J Concr Eng* 2002;24.
- [193] Jiradilok P, Nagai K, Matsumoto K. Meso-scale modeling of non-uniformly corroded reinforced concrete using 3D discrete analysis. *Eng Struct* 2019;197. <https://doi.org/10.1016/j.engstruct.2019.109378>.
- [194] Hwang YK, Lim YM. Validation of three-dimensional irregular lattice model for concrete failure mode simulations under impact loads. *Eng Fract Mech* 2017;169:109–27. <https://doi.org/10.1016/j.engfracmech.2016.11.007>.
- [195] Vidya Sagar R, Raghu Prasad BK, Nazreen S, Singh RK. Modeling mode-I fracture process in concrete at meso-scale: Computational aspects of lattice model and a comparison between results of two dimensional lattice simulation and acoustic emission measurements. *Eng Fract Mech* 2019;210:257–78. <https://doi.org/10.1016/j.engfracmech.2018.05.044>.
- [196] Schlangen E, van Mier JGM. Experimental and numerical analysis of micromechanisms of fracture of cement-based composites. *Cem Concr Compos* 1992;14:105–18. [https://doi.org/10.1016/0958-9465\(92\)90004-F](https://doi.org/10.1016/0958-9465(92)90004-F).
- [197] Jívkov AP, Engelberg DL, Stein R, Petkovski M. Pore space and brittle damage evolution in concrete. *Eng Fract Mech* 2013;110:378–95. <https://doi.org/10.1016/j.engfracmech.2013.05.007>.
- [198] Benkemoun N, Poullaïn P, Al Khazraji H, Choinska M, Khelidj A. Meso-scale investigation of failure in the tensile splitting test: Size effect and fracture energy analysis. *Eng Fract Mech* 2016;168:224–59. <https://doi.org/10.1016/j.engfracmech.2016.09.005>.
- [199] Benkemoun N, Ibrahimbegovic A, Colliat JB. Anisotropic constitutive model of plasticity capable of accounting for details of meso-structure of two-phase composite material. *Comput Struct* 2012;90–91:153–62. <https://doi.org/10.1016/j.compstruc.2011.09.003>.
- [200] Karavelić E, Nikolić M, Ibrahimbegovic A, Kurtović A. Concrete meso-scale model with full set of 3D failure modes with random distribution of aggregate and cement phase. Part I: Formulation and numerical implementation. *Comput Methods Appl Mech Eng* 2019;344:1051–72. <https://doi.org/10.1016/j.cma.2017.09.013>.
- [201] Grassl P, Grégoire D, Rojas Solano L, Pijaudier-Cabot G. Meso-scale modelling of the size effect on the fracture process zone of concrete. *Int J Solids Struct* 2012;49:1818–27. <https://doi.org/10.1016/J.IJSOLSTR.2012.03.023>.
- [202] Guo L-P, Carpinteri A, Roncella R, Spagnoli A, Sun W, Vantadori S. Fatigue damage of high performance concrete through a 2D mesoscopic lattice model. *Comput Mater Sci* 2009;44:1098–106. <https://doi.org/10.1016/J.COMMATSCL.2008.07.030>.
- [203] Grassl P, Davies T. Lattice modelling of corrosion induced cracking and bond in reinforced concrete. *Cem. Concr. Compos.* 2011;33:918–24. <https://doi.org/10.1016/j.cemconcomp.2011.05.005>.
- [204] Rezakhani R, Zhou X, Cusatis G. Adaptive multiscale homogenization of the lattice discrete particle model for the analysis of damage and fracture in concrete. *Int J Solids Struct* 2017;125:50–67. <https://doi.org/10.1016/j.ijsolstr.2017.07.016>.
- [205] Feng J, Yao W, Li W, Li W. Lattice discrete particle modeling of plain concrete perforation responses. *Int J Impact Eng* 2017;109:39–51. <https://doi.org/10.1016/j.ijimpeng.2017.05.017>.
- [206] Cusatis G, Mencarelli A, Pelessone D, Baylot J. Lattice Discrete Particle Model (LDPM) for failure behavior of concrete. II: Calibration and validation. *Cem Concr Compos* 2011;33:891–905. <https://doi.org/10.1016/j.cemconcomp.2011.02.010>.
- [207] Van Mier JGM, Van Vliet MRA, Wang TK. Fracture mechanisms in particle composites: Statistical aspects in lattice type analysis. *Mech Mater* 2002;34:705–24. [https://doi.org/10.1016/S0167-6636\(02\)00170-9](https://doi.org/10.1016/S0167-6636(02)00170-9).
- [208] Grassl P. A lattice approach to model flow in cracked concrete. *Cem Concr Compos* 2009;31:454–60. <https://doi.org/10.1016/j.cemconcomp.2009.05.001>.
- [209] Sadouki H, Van Mier JGM. Meso-level analysis of moisture flow in cement composites using a lattice-type approach. *Mater Struct Constr* 1997;30:579–87. <https://doi.org/10.1007/bf02486899>.
- [210] Benkemoun N, Hammoud MN, Amiri O. Embedded finite element formulation for the modeling of chloride diffusion accounting for chloride binding in meso-scale concrete. *Finite Elem Anal Des* 2017;130:12–26. <https://doi.org/10.1016/j.finel.2017.03.003>.
- [211] Šavija B, Pacheco J, Schlangen E. Lattice modeling of chloride diffusion in sound and cracked concrete. *Cem Concr Compos* 2013;42:30–40. <https://doi.org/10.1016/j.cemconcomp.2013.05.003>.
- [212] Šavija B, Luković M, Schlangen E. Lattice modeling of rapid chloride migration in concrete. *Cem Concr Res* 2014;61–62:49–63. <https://doi.org/10.1016/j.cemconres.2014.04.004>.
- [213] Abdellatif M, Boumakis I, Wan-Wendner R, Alnaggard M. Lattice Discrete Particle Modeling of concrete coupled creep and shrinkage behavior: A comprehensive calibration and validation study. *Constr Build Mater* 2019;211:629–45. <https://doi.org/10.1016/j.conbuildmat.2019.03.176>.
- [214] Boumakis I, Di Luzio G, Marcon M, Vorel J, Wan-Wendner R. Discrete element framework for modeling tertiary creep of concrete in tension and compression. *Eng Fract Mech* 2018;200:263–82. <https://doi.org/10.1016/j.engfracmech.2018.07.006>.
- [215] Zhou R, Lu Y. A mesoscale interface approach to modelling fractures in concrete for material investigation. *Constr Build Mater* 2018;165:608–20. <https://doi.org/10.1016/j.conbuildmat.2018.03.070>.

- org/10.1016/J.CONBUILDMAT.2018.01.040.
- [216] Schlangen E, Garboczi EJ. New method for simulating fracture using an elastically uniform random geometry lattice. *Int J Eng Sci* 1996;34:1131–44. [https://doi.org/10.1016/0020-7225\(96\)00019-5](https://doi.org/10.1016/0020-7225(96)00019-5).
- [217] Kristombu Baduge Shanaka, Mendis Priyan, Ngo Tuan, Portella Joanne, Nguyen Kate. Understanding failure and stress-strain behavior of very-high strength concrete (> 100 MPa) confined by lateral reinforcement. *Constr Build Mater* 2018;189:62–77. <https://doi.org/10.1016/J.CONBUILDMAT.2018.08.192> In this issue.
- [218] Kristombu Baduge Shanaka, Mendis Priyan, Ngo Tuan. Stress-strain relationship for very-high strength concrete (> 100 MPa) confined by lateral reinforcement. *Eng Struct* 2018;177:795–808. <https://doi.org/10.1016/J.ENGSTRUCT.2018.08.008> In this issue.
- [219] Kristombu Baduge Shanaka, Mendis Priyan, Ngo Tuan, Sofi Massoud. Ductility design of reinforced very-high strength concrete columns (100–150 MPa) using curvature and energy-based ductility indices. *Int J Concr Struct Mater* 2019;13(1):37. <https://doi.org/10.1186/s40069-019-0347-y> In this issue.
- [220] Kristombu Baduge Shanaka, Mendis Priyan. Novel energy-based rational for nominal ductility design of very-high strength concrete columns (> 100 MPa). *Eng Struct* 2019;198. <https://doi.org/10.1016/j.engstruct.2019.109497> In this issue.
- [221] Baduge Shanaka Kristombu, Mendis Priyan, San Nicolas Rackel, Rupasinghe Maduwanthi, Portella Joanne. Aggregate-dependent approach to formulate and predict properties of high-strength and very-high-strength concrete. *J Mat Civ Eng* 2020;32(4). [https://doi.org/10.1061/\(ASCE\)MT.1943-5533.0003055](https://doi.org/10.1061/(ASCE)MT.1943-5533.0003055) In this issue.